

Supplementary material for the article:

Chen, J.; Unjaroen, D.; Stepanovic, S.; Van Dam, A.; Gruden, M.; Browne, W. R. Selective Photo-Induced Oxidation with O₂ of a Non-Heme Iron(III) Complex to a Bis(Imine-Pyridyl)Iron(II) Complex. *Inorganic Chemistry* 2018, 57 (8), 4510–4515.

<https://doi.org/10.1021/acs.inorgchem.8b00187>

Supplementary information

Selective Photo-Induced Oxidation with O₂ of a Non-Heme Iron(III) Complex to a Bis-(imine- pyridyl)Iron (II) Complex

Juan Chen,[†] Duenpen Unjaroen,[†] Stepan Stepanovic,[‡] Annie van Dam,[§] Maja Gruden,^{‡}
Wesley R. Browne^{*†}*

[†] Stratingh Institute for Chemistry, Faculty of Science and Engineering, University of Groningen, Nijenborgh 4, 9747AG, Groningen, The Netherlands

[‡] Faculty of Chemistry, University of Belgrade, Studentski trg 12–16, 11000 Belgrade, Serbia.

[§] Interfaculty Mass Spectrometry Center, University of Groningen, Groningen, the Netherlands

KEYWORDS. Photochemistry, non-heme iron complex, oxygen, isomerization, spectroscopy.

Table of Contents

1. Experimental Details	3
2. Additional Figures and Schemes	5
a. NMR Analysis Section.....	11
b. Computational section.....	20
Computational details:	20
Results and discussion:.....	20
c. Mechanistic considerations	22
d. Coordinates and electronic energies (in <i>kcal/mol</i>) of all optimized structures	26
3. References	32

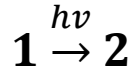
1. Experimental Details

1,1-di(pyridin-2-yl)-N,N-bis(pyridin-2-ylmethyl)ethan-1-amine (MeN4Py),¹ complexes [(MeN4Py)Fe^{III}(OCH₃)](ClO₄)₂¹ (**1**) and [(MeN4Py)Fe^{II}(CH₃CN)](ClO₄)₂² (**3**), [(N4Py)Fe^{III}(OMe)](ClO₄)₂³ (**2**)³ were prepared as reported previously. [(MeN4Py)Fe^{II}(OCH₃)]⁺ (**1a**) was generated by dissolving [(MeN4Py)Fe^{II}(CH₃CN)](ClO₄)₂¹ (**3**) in methanol.⁴ Commercially available chemicals were purchased from Sigma Aldrich without further purification. All solvents used for spectroscopy were of UVASOL (Merck) grade. [(MeN4Py)Fe^{III}(Cl)](ClO₄)₂ (**1-Cl**) was prepared by mixing equimolar amounts of Fe^{III}Cl₃ and the ligand (Men4py) in acetonitrile, followed by addition of 10 equiv. NaClO₄ in a minimum amount of acetonitrile. Vapour diffusion of diethyl ether into the solution at room temperature provided signal crystals of [(MeN4Py)Fe^{III}(Cl)](ClO₄)₂.

Irradiation Typically 2 mL of **1-3** (0.125 mM) in solvent were purged with Ar in a 1 cm path length cuvette for 5 min before irradiation to remove oxygen. Irradiation was carried out orthogonally to the monitoring beam of the UV-vis absorption spectrometer. LEDs (Thorlabs) were used at 365 nm (M365 F1, 6.10×10^{-5} einstein s⁻¹ dm⁻³), 490 nm (M490F3, 4.76×10^{-6} einstein s⁻¹ dm⁻³), 565 nm (M565F, 3.19×10^{-6} einstein s⁻¹ dm⁻³), and 300 nm (M300F2, 1.25×10^{-6} einstein s⁻¹ dm⁻³) controlled by T-Cube Light Source & Driver Module (Thorlabs); or a DPSS laser at 355 nm (9.79×10^{-6} einstein s⁻¹ dm⁻³, Cobolt Lasers). Light intensity at sample was measured with PM10V1 High Power 10 Watt sensor coupled to a FieldMate Power Meter.

Quantum yield measurements: The photon flux of light sources used for quantum yield measurements was determined using the potassium ferrioxalate actinometer. The literature method⁵ was modified as described earlier.⁶ The photo conversion of **1** to **A²⁺** was calculated according to the literature procedures^{7,8} established for irreversible photochemical conversions (see below).

For the photochemical conversion from **1** to **A²⁺** (**2** is used to refer to **A²⁺** in equations for simplification),



1. Plot the decrease of absorbance of **1**, and fit the equation below, get the rate constant, $-k_1^{\lambda_{irr}}$

$$A_{tot}^{\lambda_{irr}/\lambda_{obs}}(t) = A_2^{\lambda_{irr}/\lambda_{obs}}(\infty) + \frac{A_1^{\lambda_{irr}/\lambda_{obs}}(0) - A_2^{\lambda_{irr}/\lambda_{obs}}(\infty)}{A_1^{\lambda_{irr}/\lambda_{irr}}(0) - A_2^{\lambda_{irr}/\lambda_{irr}}(\infty)} \times \log[1 + (10^{[A_1^{\lambda_{irr}/\lambda_{irr}}(0) - A_2^{\lambda_{irr}/\lambda_{irr}}(\infty)]} - 1) \times e^{-k_1^{\lambda_{irr}} \times t}]$$

in which, $A_1^{\lambda_{irr}/\lambda_{obs}}(0)$ is the absorbance of species **1** at $t = 0$ at plotting wavelength, e.g., 310 nm.

$A_2^{\lambda_{irr}/\lambda_{obs}}(\infty)$ is the absorbance of species **A²⁺** at $t = \text{end}$ at plotting wavelength e.g., 310 nm.

$A_1^{\lambda_{irr}/\lambda_{irr}}(0)$ is the absorbance of species **1** at $t = 0$ at irradiation wavelength, e.g., 365 nm.

$A_2^{\lambda_{irr}/\lambda_{irr}}(\infty)$ is the absorbance of species **A²⁺** at $t = \text{end}$ at irradiation wavelength, e.g., 365 nm.

2. The quantum yield (Φ) was calculated using equation

$$k_1^{\lambda_{irr}} = \Phi_{1 \rightarrow 2}^{\lambda_{irr}} \times \epsilon_1^{\lambda_{irr}} \times l_{\lambda_{irr}} \times P_{\lambda_{irr}} \times F_{\infty}^{\lambda_{irr}}$$

and then

$$\Phi_{1 \rightarrow 2}^{\lambda_{irr}} = k_1^{\lambda_{irr}} / (\epsilon_1^{\lambda_{irr}} \times l_{\lambda_{irr}} \times P_{\lambda_{irr}} \times F_{\infty}^{\lambda_{irr}})$$

In which $F_{\infty}^{\lambda_{irr}}$.

$$F_{\infty}^{\lambda_{irr}} = \frac{1 - 10^{-[A_2^{\lambda_{irr}/\lambda_{irr}}(\infty)]}}{A_2^{\lambda_{irr}/\lambda_{irr}}(\infty)}$$

and $P_{\lambda_{irr}}$ (einstein s⁻¹ dm⁻³) is obtained from actinometry, $l_{\lambda_{irr}}$ is the cuvette path length (1 cm), $\epsilon_1^{\lambda_{irr}}$ is the absorption coefficient of complex **1** in irradiation wavelength.

2. Additional Figures and Schemes

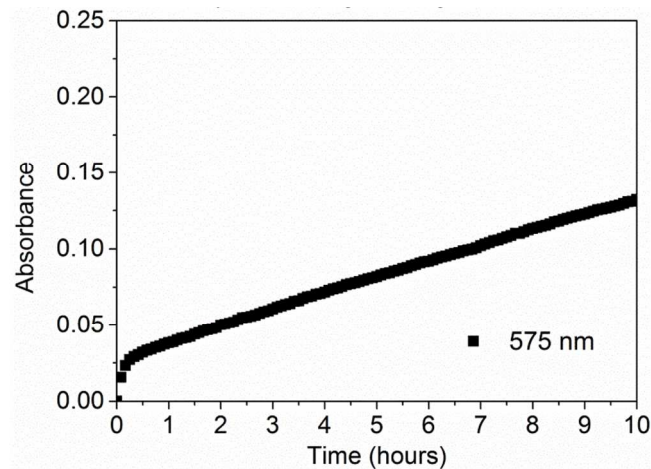


Figure S 1. Absorbance of **1** (0.125 mM) in methanol with 50 equiv. Et₃N at 575 nm over time (without irradiation - a JASCO V-570 UV/Vis-NIR spectrometer at a single wavelength was employed to avoid photochemically induced changes).

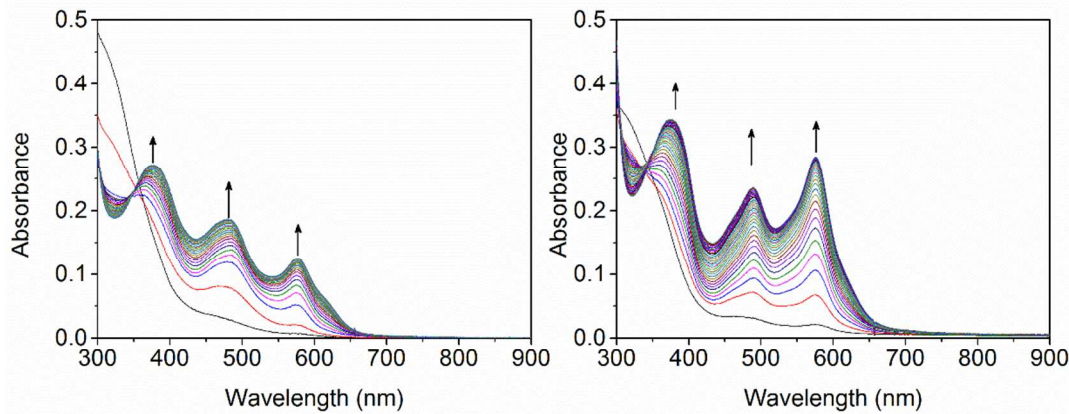


Figure S 2. UV-vis spectrum of **1** in air equilibrated methanol before (black) and under irradiation (λ_{exc} 365 nm) with (left) 50 equiv. and (right) 250 equiv. of NaOAc.

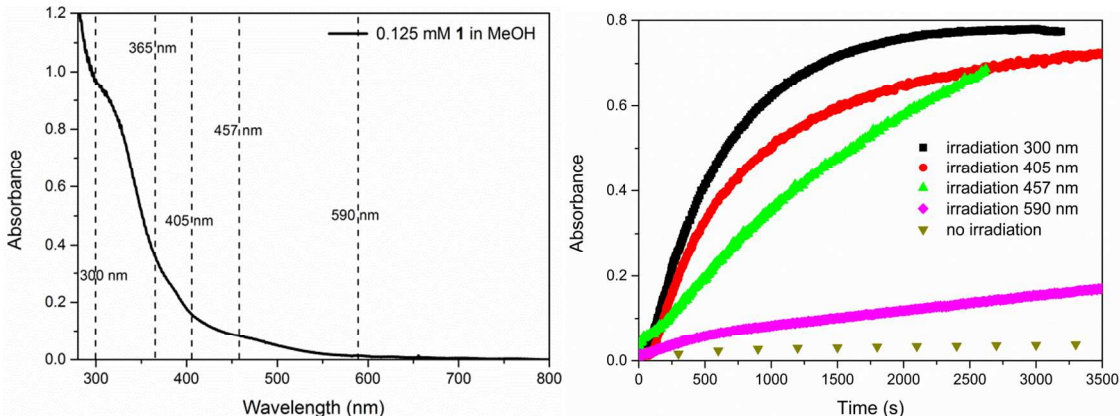


Figure S 3. (left) Correspondence of irradiation wavelengths used with the UV-Vis absorption spectrum of **1** in methanol and (right) absorbance at 575 nm over time showing the photochemical conversion of **1** to **A²⁺** with 50 equiv. Et₃N (irradiation commenced 5 min after addition of Et₃N in each case). The rate of conversion is less at 590 nm due primarily to the low molar absorptivity of **1** at this wavelength and overlap with more intense absorption of **A²⁺** and **1a** (manifested in a observed quantum yield at 590 nm of < 0.001)

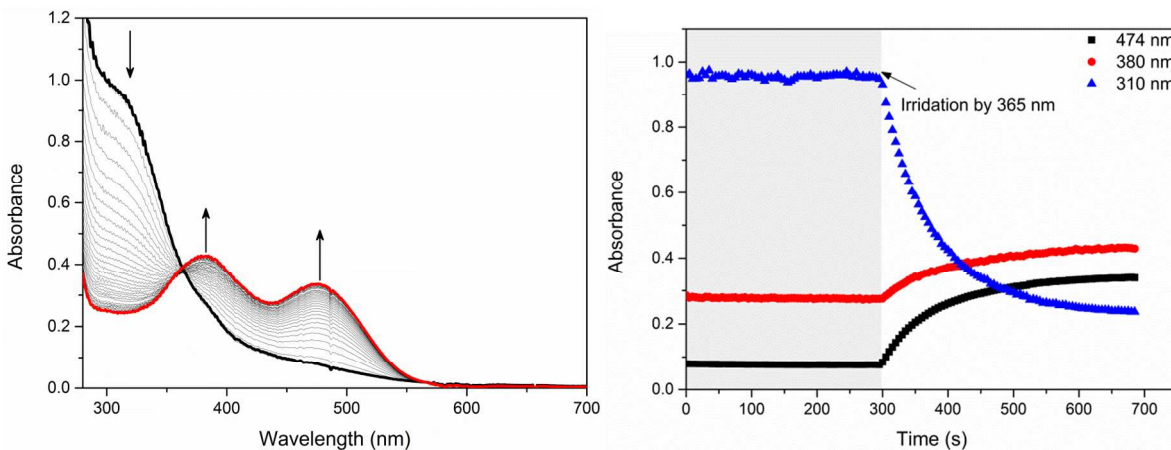


Figure S 4. (Left) UV/Vis absorption spectrum of **1** (0.125 mM, black) with 50 equiv. Et₃N in argon purged methanol and under irradiation at 365 nm. Final spectrum shown in red. (Right) Absorbance at 474, 380 and 310 nm, before and during irradiation at 365 nm.

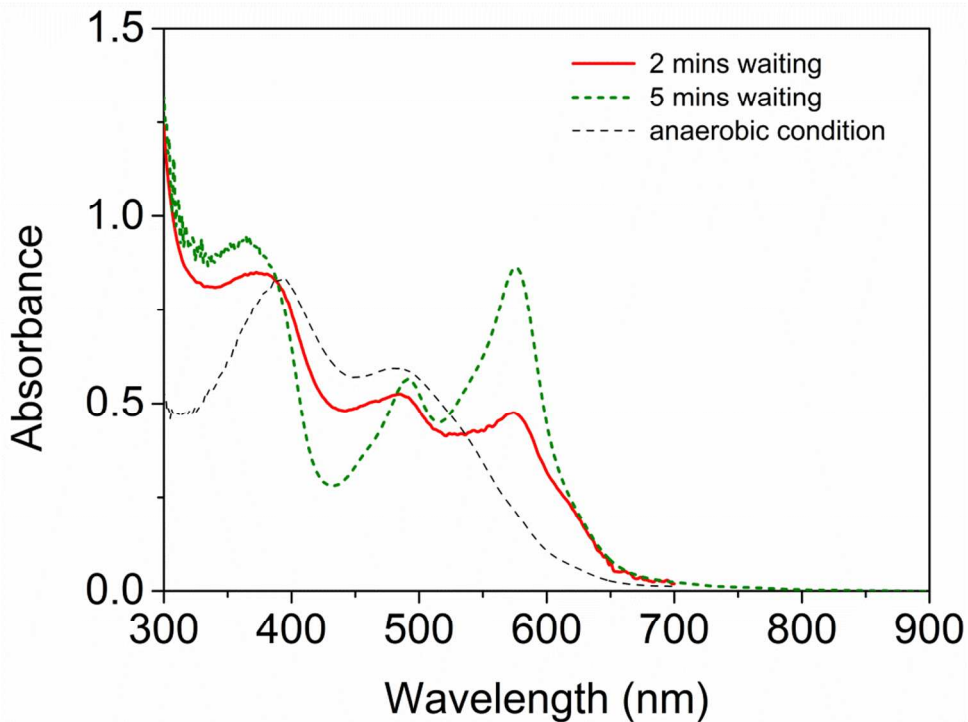


Figure S 5. UV-vis spectra of the reaction mixture of **1** (0.25 mM) in methanol with 50 equiv. Et_3N after irradiation ($\lambda = 365 \text{ nm}$), (red) irradiation commenced 2 minutes after addition of Et_3N , (black) irradiation commenced 5 minutes after addition of Et_3N , (green) irradiation commenced immediately after addition of Et_3N .

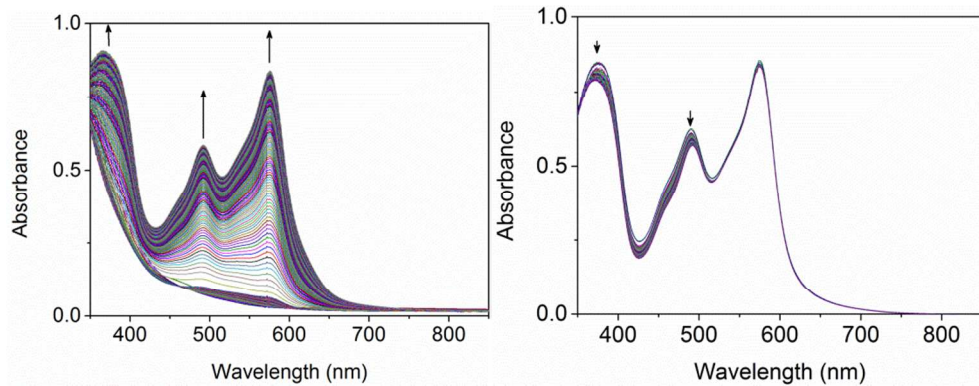
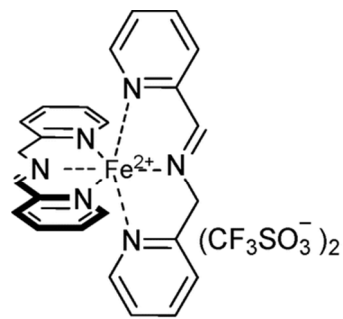


Figure S 6. (left) UV-vis spectrum of **1** (0.25 mM) in methanol with 50 equiv. Et_3N during irradiation ($\lambda = 365 \text{ nm}$, irradiation commenced 5 min after addition of Et_3N), (right) addition of 50 equiv. H_2O_2 to the solution after irradiation (the minor decrease at 380 and 490 nm due to reaction of H_2O_2 with residual $[(\text{MeN}_4\text{Py})\text{Fe}^{\text{II}}\text{OCH}_3]^{2+}$ formed in competition with formation of A^{2+}).



Scheme S 1. Bis-tridentate immine-based iron(II) complex ($\mathbf{B}^{2+}\text{-OTf}$) reported by Di Stefano et. al.⁹

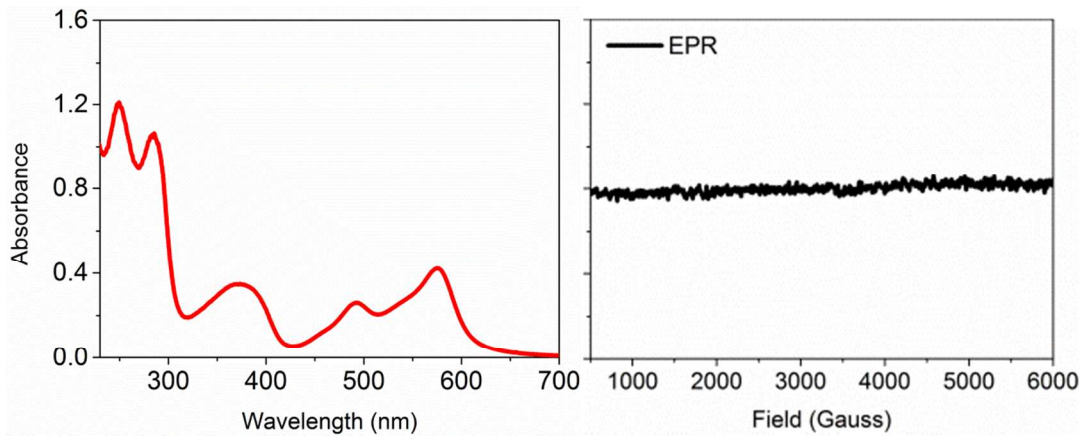


Figure S 7. (Left) UV/Vis absorption spectrum of photo-product \mathbf{A}^{2+} in methanol (Right) X-band EPR spectrum at 77 K of \mathbf{A}^{2+} in methanol.

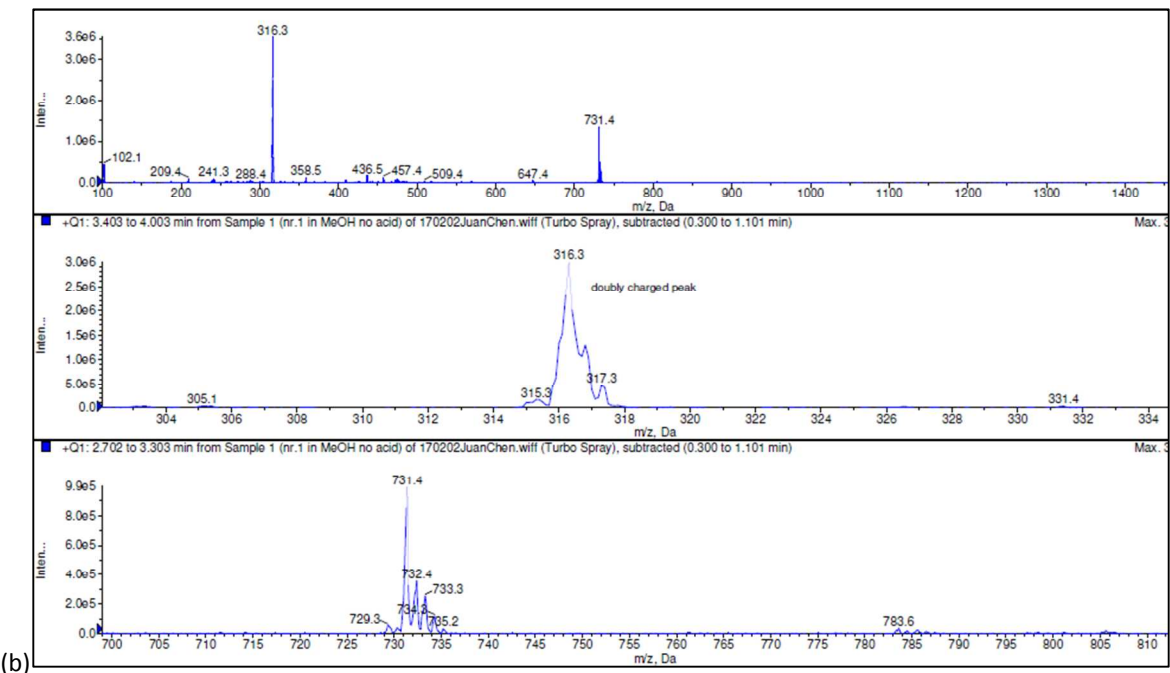
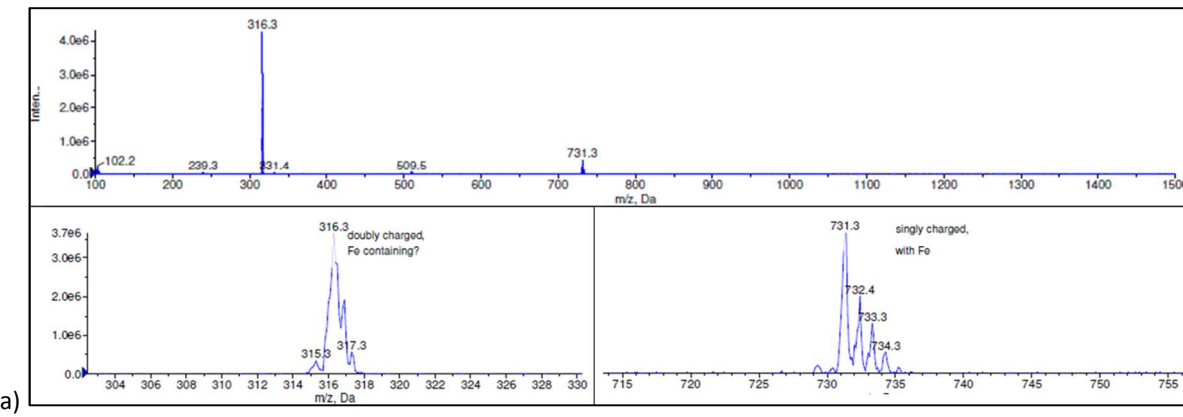


Figure S 8. ESI/MS spectra of \mathbf{A}^{2+} in acetonitrile (a) and in methanol (b).

Resonance Raman spectra of **A**²⁺ (Figure S9) in methanol at λ_{exc} 561 nm were compared with a freshly prepared imine-based Fe^{II} complex (**B**²⁺, Scheme S1). The bands at 651, 681, 956, 1226, 1468, 1551, 1554, 1581, and 1609 cm⁻¹ are resonantly enhanced in the spectrum of **A**²⁺ and are similar to those of **B**²⁺, except for a 10 cm⁻¹ shift at 651 and 1581 cm⁻¹ to lower wavenumbers, which is consistent with the presence of an extra pyridine and methyl group in **A**²⁺ compared to complex **B**²⁺. The band at 1551 cm⁻¹ is assigned to a C=N stretching mode using DFT calculations with anharmonic correction.

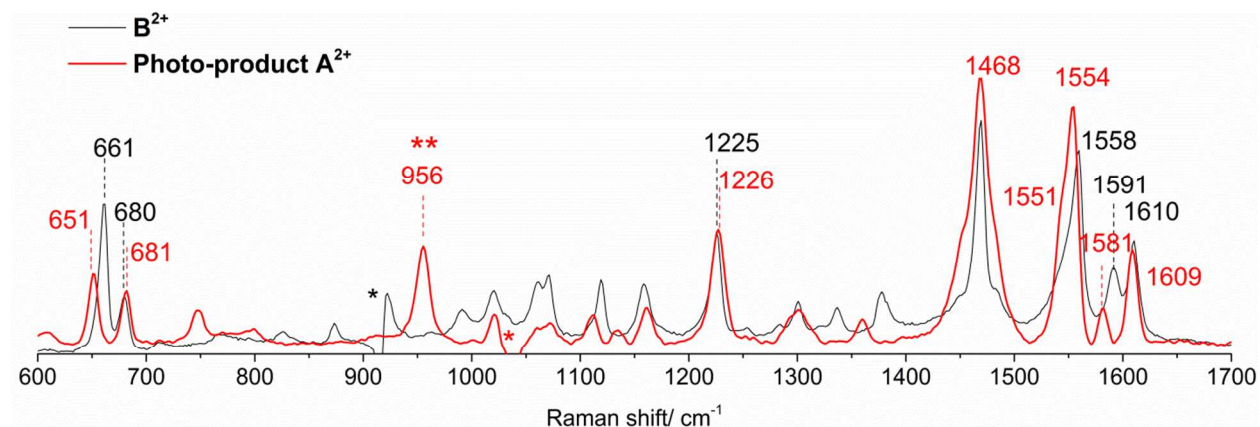


Figure S 9. Resonance Raman spectra at λ_{exc} 561 nm of photo-product **A**²⁺ in methanol (red) with **B**²⁺ in acetonitrile (black). (*) artifacts due to imperfect solvent subtraction, (**) ClO₄⁻.

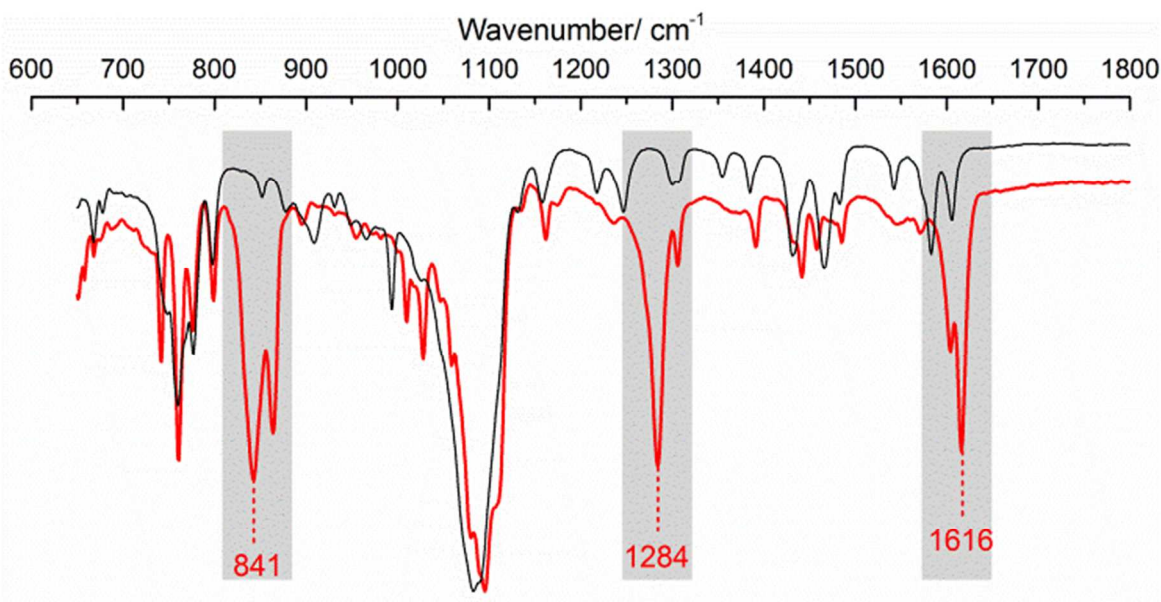


Figure S 10. FTIR spectra of the obtained precipitates during the photochemical oxidation of **1** to **A**²⁺ (red) and photo-product **A**²⁺ (black).

a. NMR Analysis Section

¹H NMR of photo product at 75 °C, (400 MHz, CD₃CN) δ 10.76 (s, 1H, imine-H), 8.29 (d, *J* = 7.6 Hz, 1H), 7.89 (d, *J* = 7.6 Hz, 1H), 7.84 (t, *J* = 7.6 Hz, 1H), 7.75 (t, *J* = 7.6 Hz, 1H), 7.50 (d, *J* = 8.0 Hz, 1H), 7.45 (s, br, 1H), 7.26-7.31 (br, 2H), 7.24, (d, *J* = 8.0 Hz, 2H), 7.11 (br, 1H), 2.93 (s, 3H, -CH₃). ¹³C NMR (101 MHz, CD₃CN) δ 173.9, 161.6, 156.4, 154.1, 141.2, 141.0, 140.6, 132.3, 130.1, 127.3, 127.3, 126.3, 126.1, 83.4, 33.2.

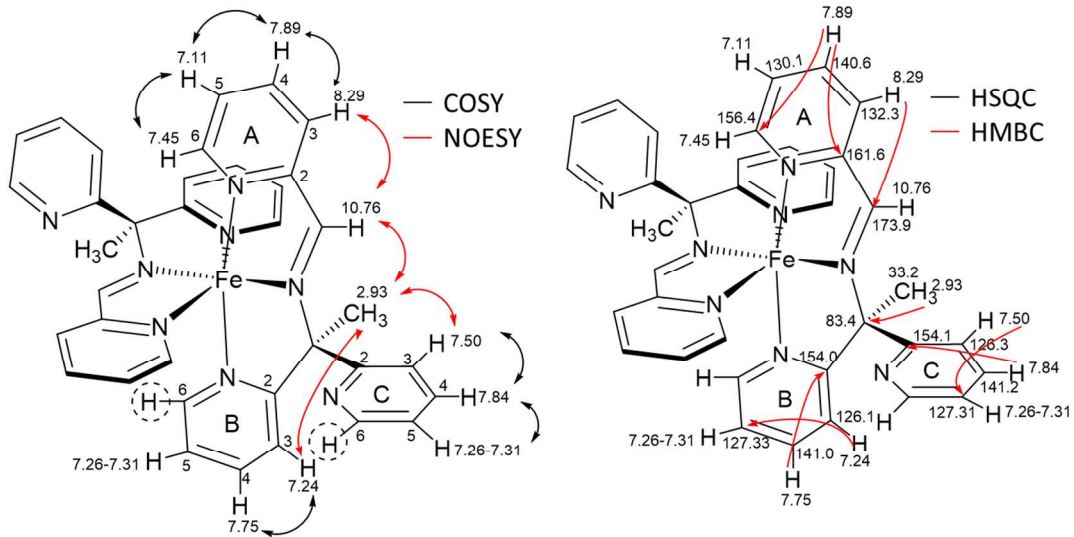


Figure S 11. 2D NMR characterization of **A**²⁺ in acetonitrile-*d*₃ at 75 °C

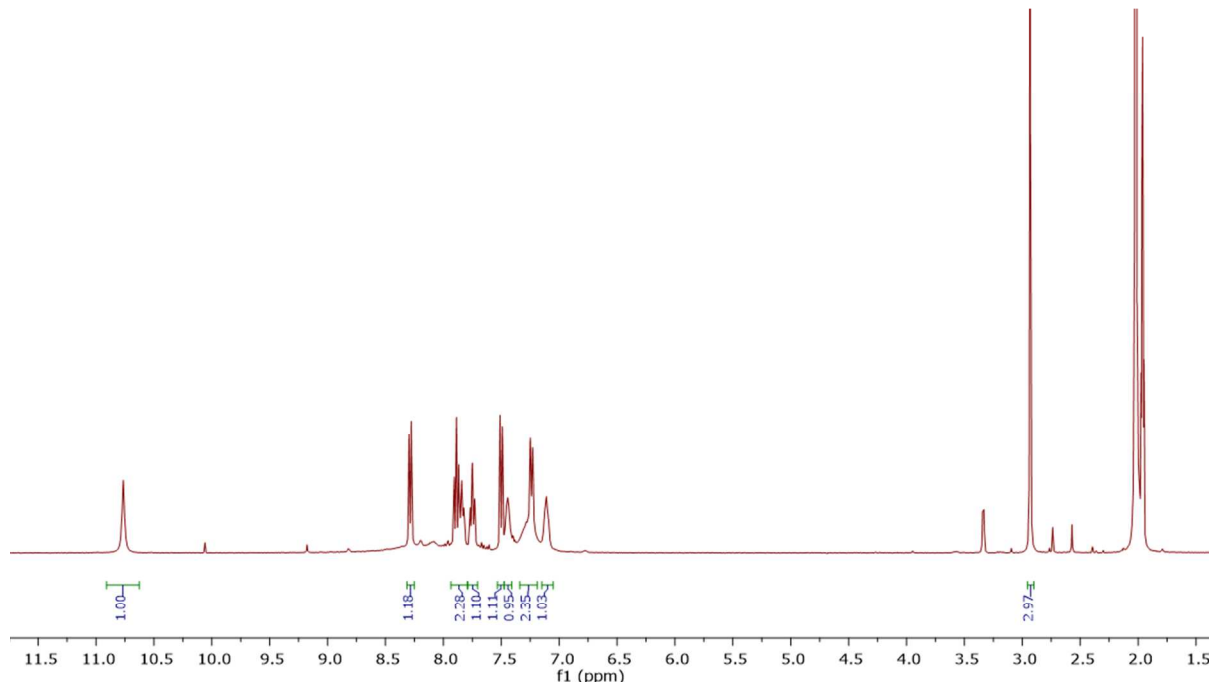


Figure S 12. ¹H NMR spectrum of **A**²⁺ in acetonitrile-*d*₃ at 75 °C.

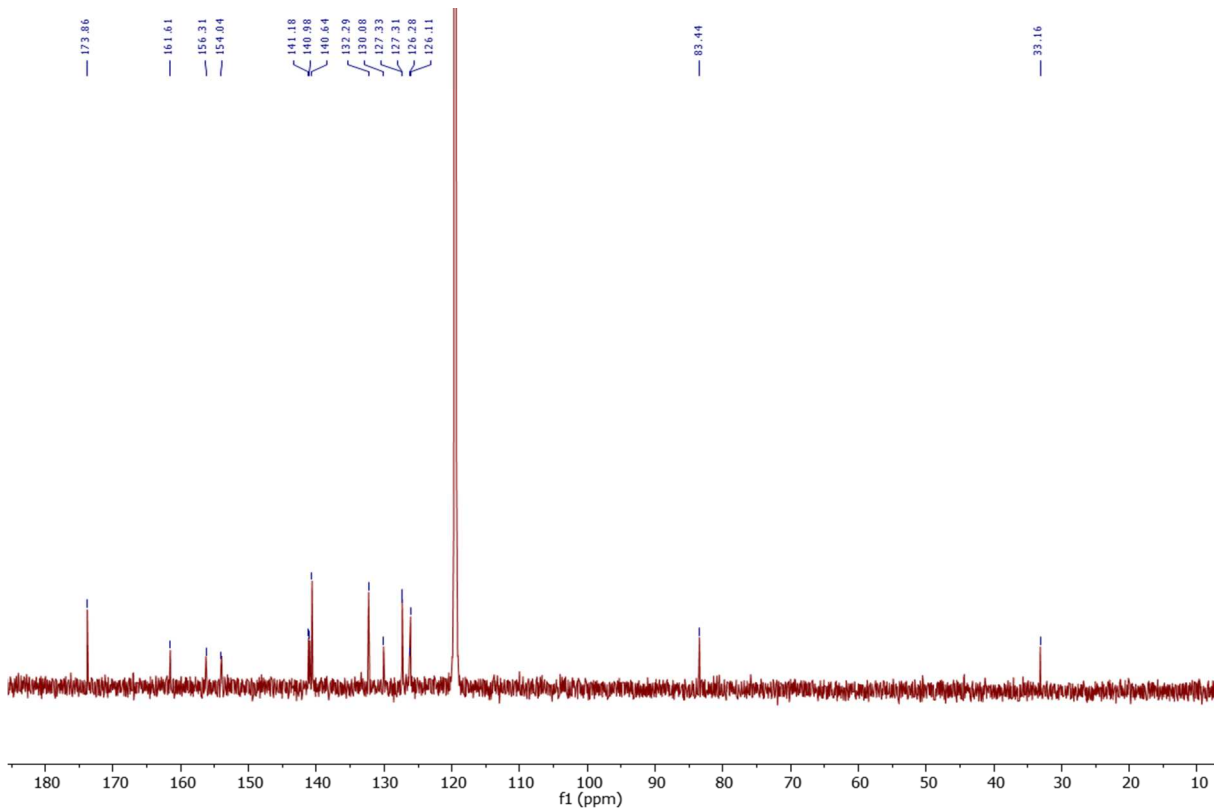


Figure S 13. ^{13}C NMR spectrum of \mathbf{A}^{2+} in acetonitrile- d_3 at 75 °C.

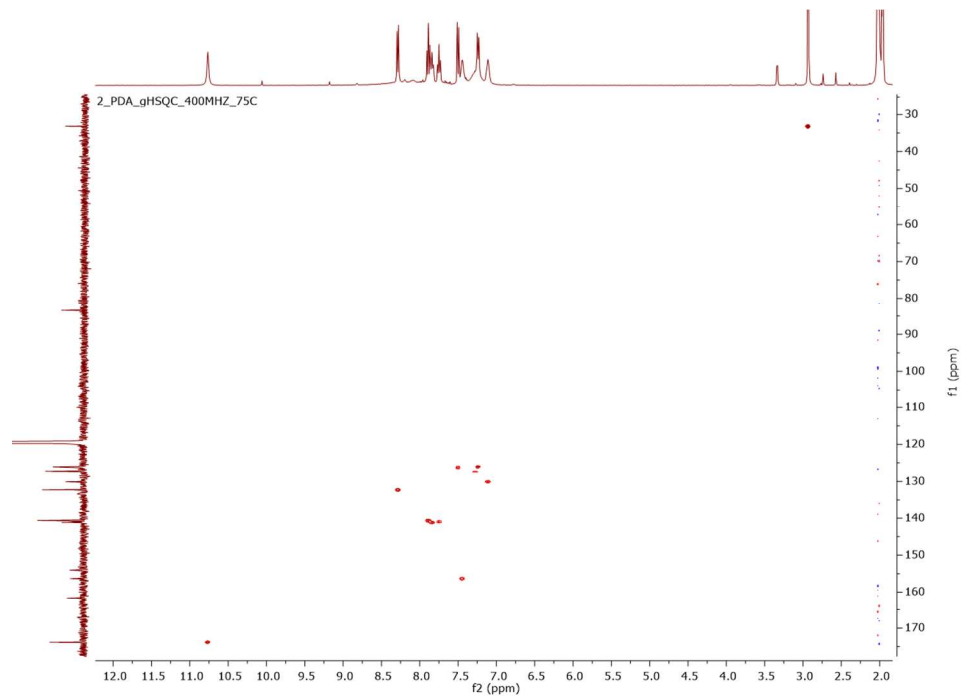


Figure S 14. HSQC NMR spectrum of \mathbf{A}^{2+} in acetonitrile- d_3 at 75 °C.

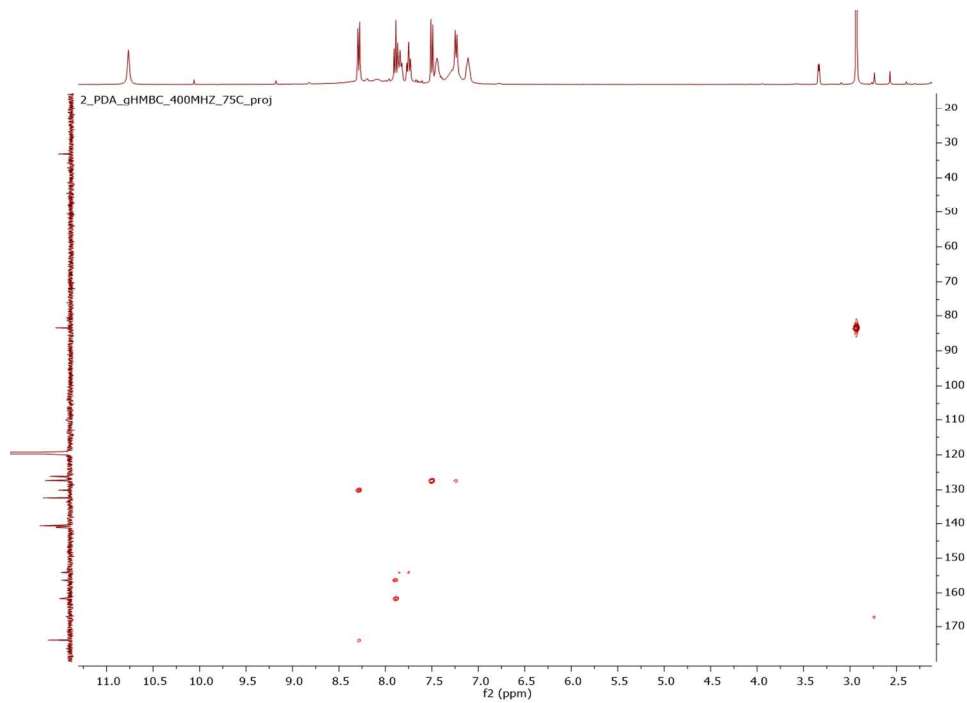


Figure S 15. HMBC NMR spectrum of \mathbf{A}^{2+} in acetonitrile- d_3 at 75 °C

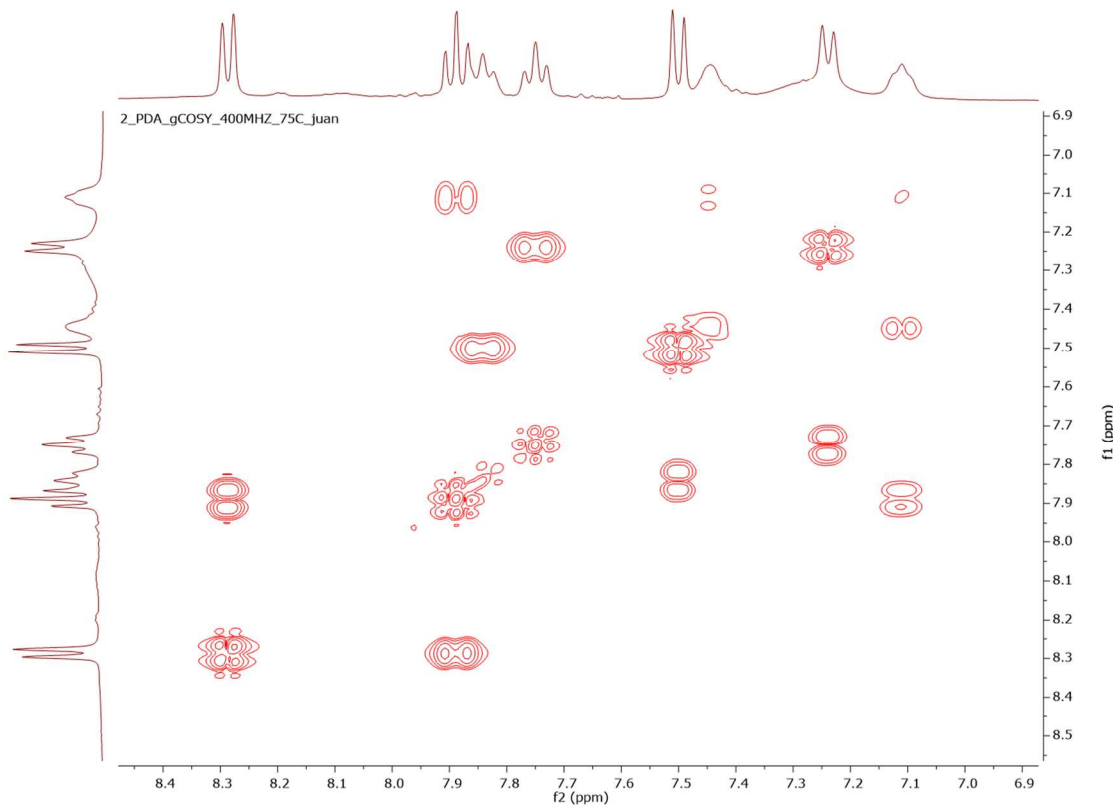


Figure S 16. ^1H COSY NMR spectrum of \mathbf{A}^{2+} in acetonitrile- d_3 at 75 °C.

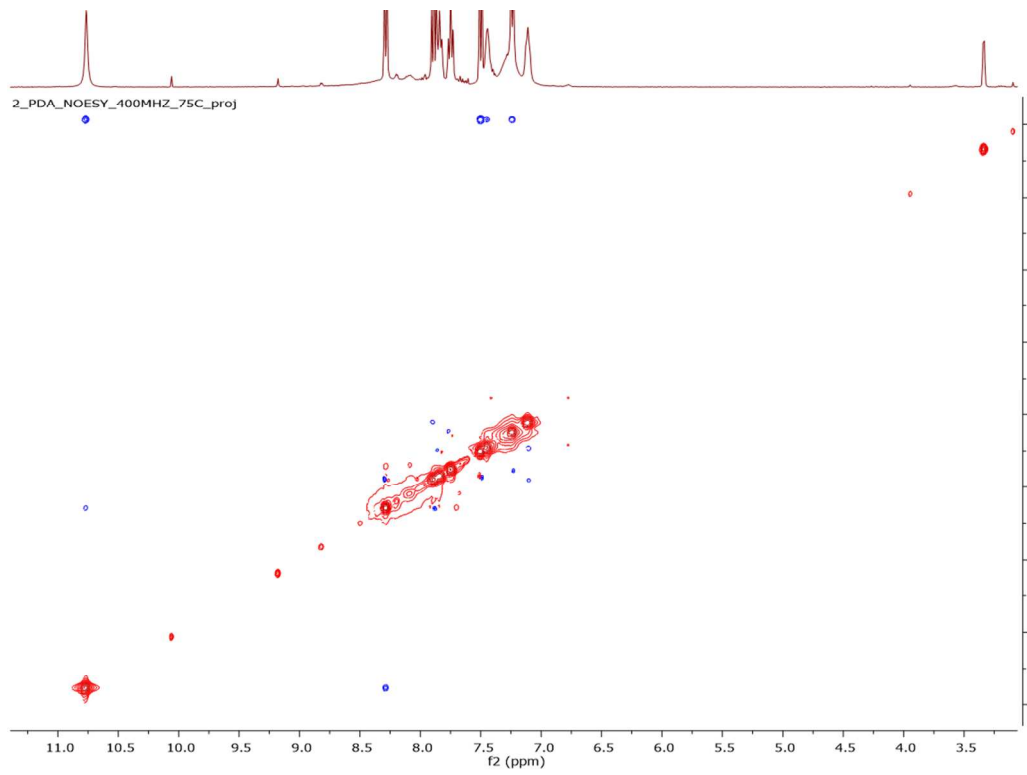


Figure S 17. ^1H - ^1H NOESY NMR spectrum of \mathbf{A}^{2+} in acetonitrile- d_3 at 75 °C.

At -30 °C, the integration of photo product corresponds to 64 H of a mixture of four isomers in the ratio 1:1.2:0.8:1, each of which show C₂ symmetry. The ¹³C NMR spectrum is consistent to four isomers (72 C) with 4 carbons corresponding to a methyl group at 32 and 33 ppm and 16 signals of quaternary carbon at 83, 161, 162, 171 and 172 ppm (Figure S24). 2D NMR techniques (HSQC, HMBC, COSY and NOESY) were used in the assignment of (conformational) isomers of the photo product.

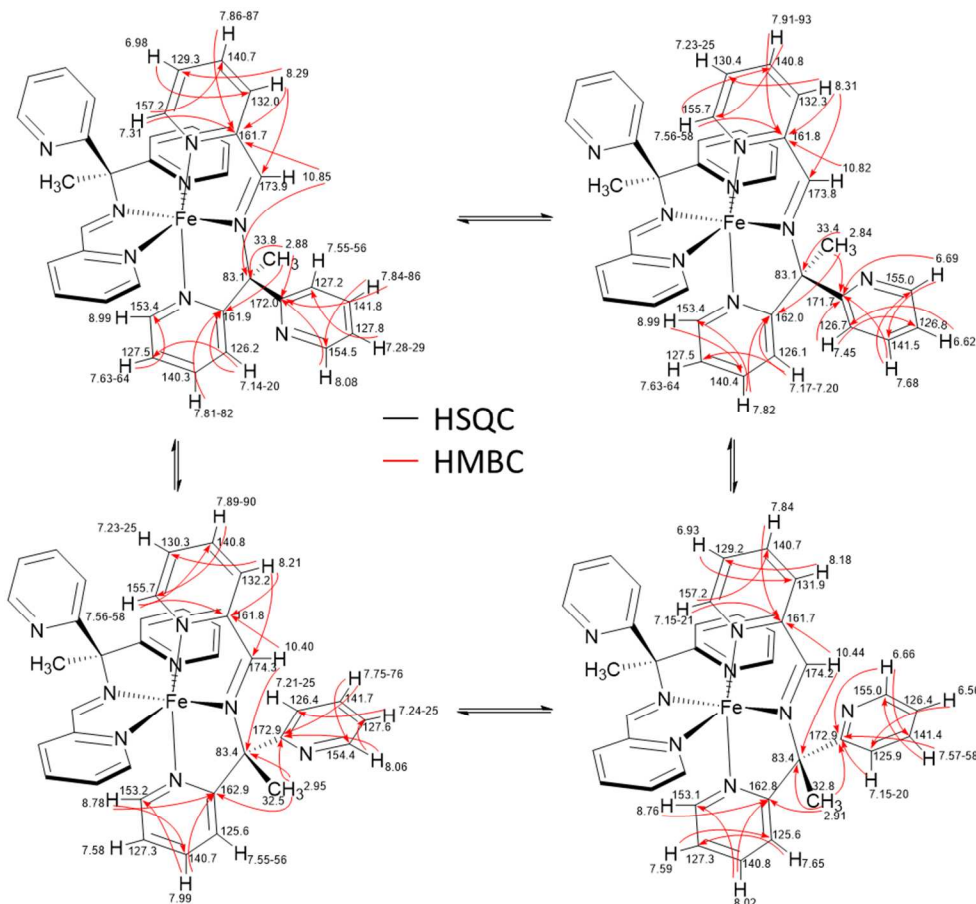


Figure S 18. 2D NMR (HSQC and HMBC) characterization of **A²⁺** in acetonitrile-*d*₃ at -30 °C

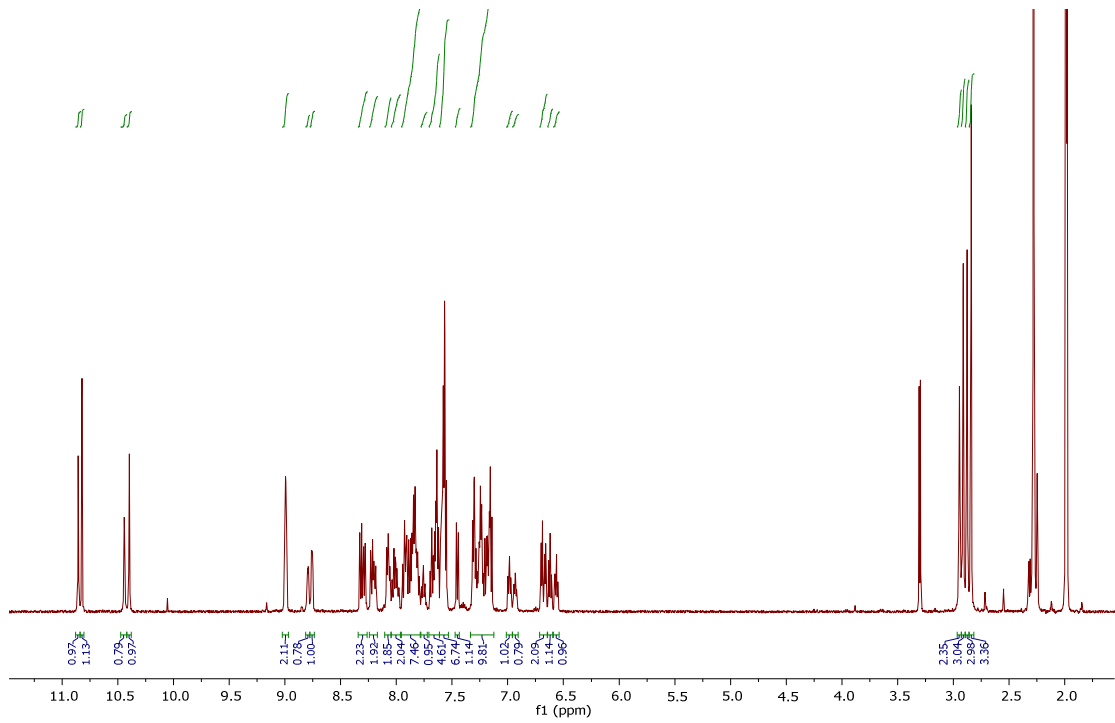


Figure S 19. ^1H NMR spectrum of \mathbf{A}^{2+} in acetonitrile- d_3 at -30°C.

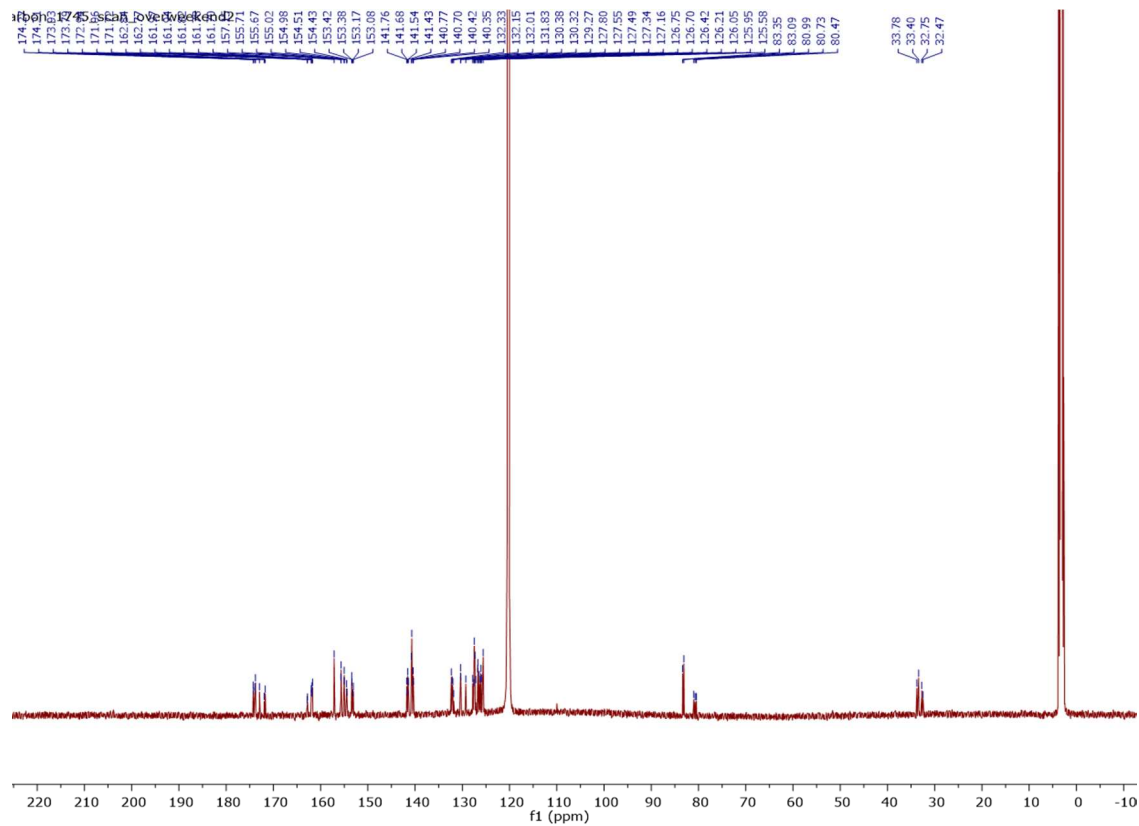


Figure S 20. ^{13}C NMR spectrum of \mathbf{A}^{2+} in acetonitrile- d_3 at -30°C.

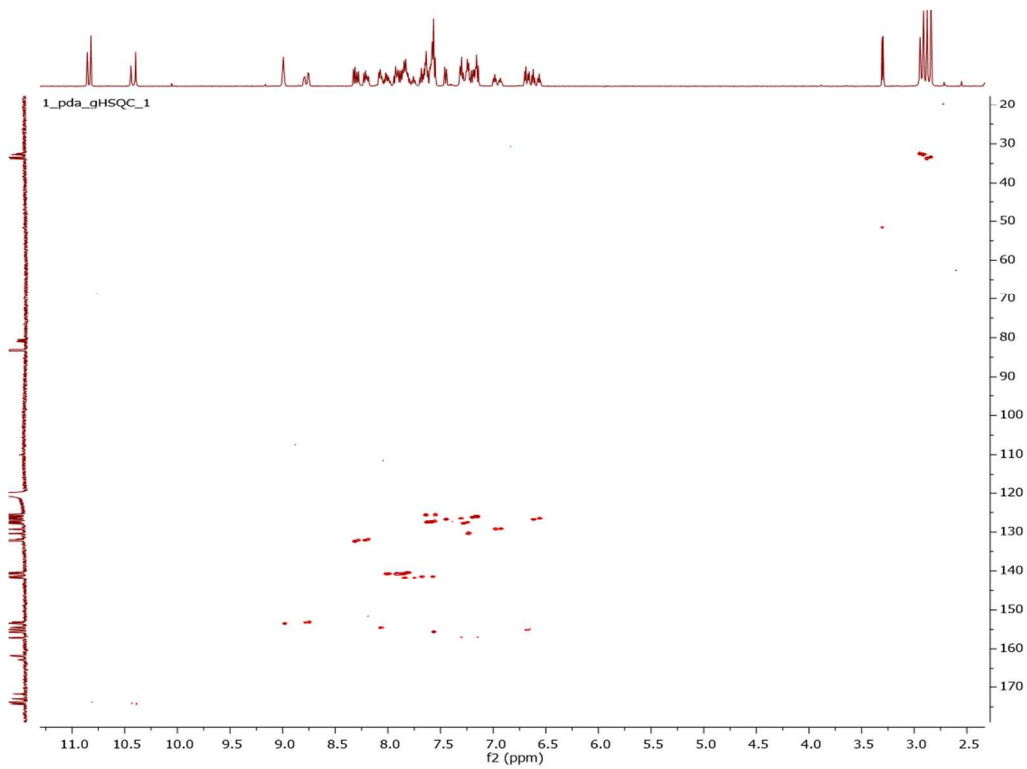


Figure S 21 HSQC NMR spectrum of **A**²⁺ in acetonitrile-*d*₃ at -30 °C.

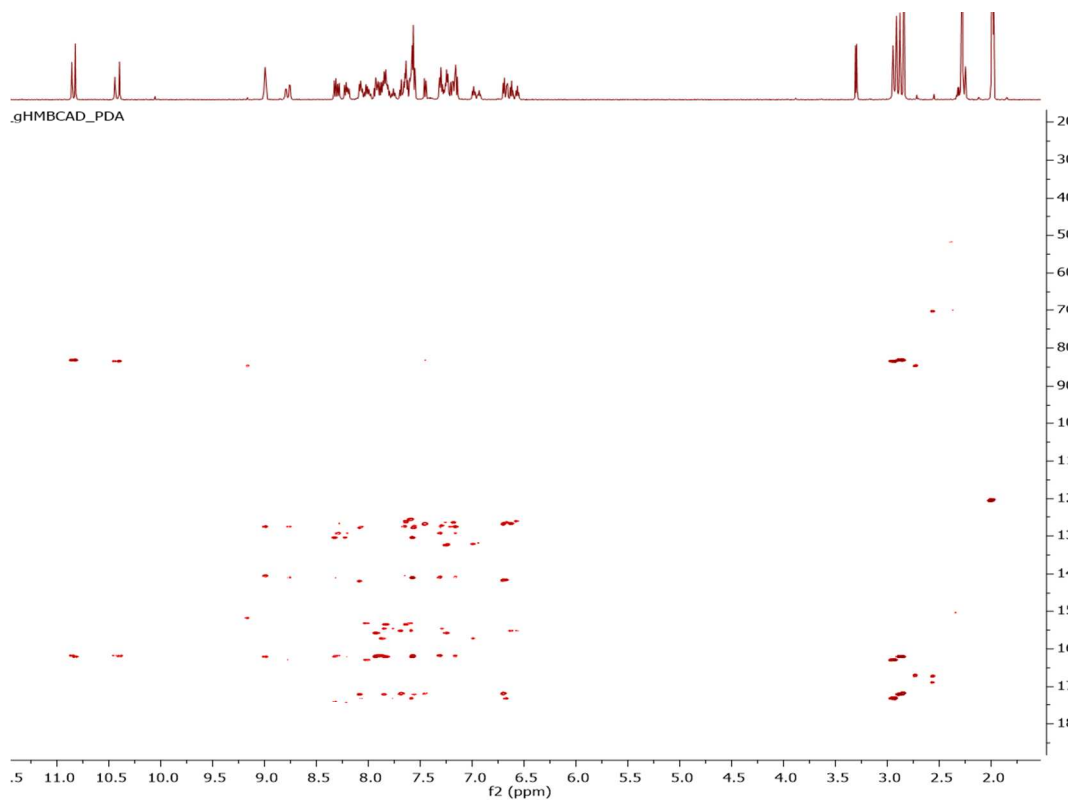


Figure S 22. HMBC NMR spectrum of **A**²⁺ in acetonitrile-*d*₃ at -30 °C.

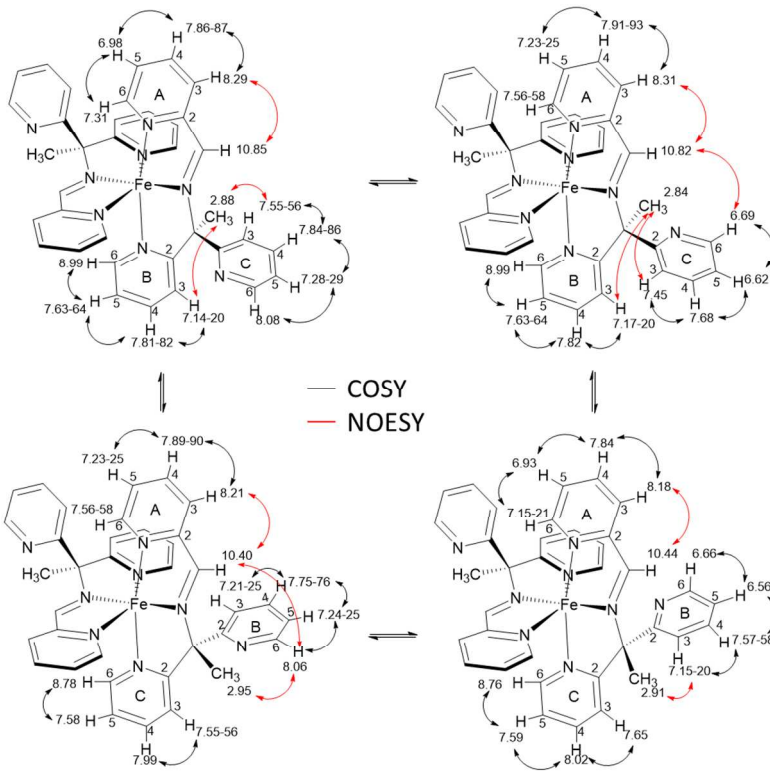


Figure S 23. 2D NMR (COSY NOESY) characterization of \mathbf{A}^{2+} in acetonitrile- d_3 at $-30\text{ }^\circ\text{C}$

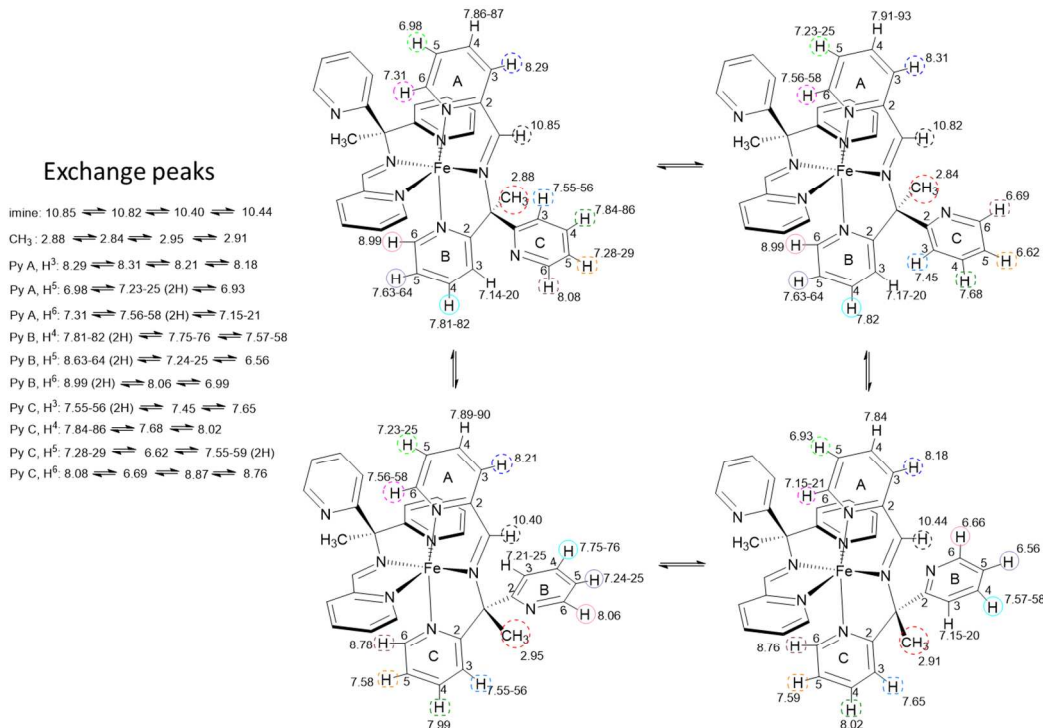


Figure S 24. 2D NOESY (exchange peaks) characterization of \mathbf{A}^{2+} in acetonitrile- d_3 at $-30\text{ }^\circ\text{C}$

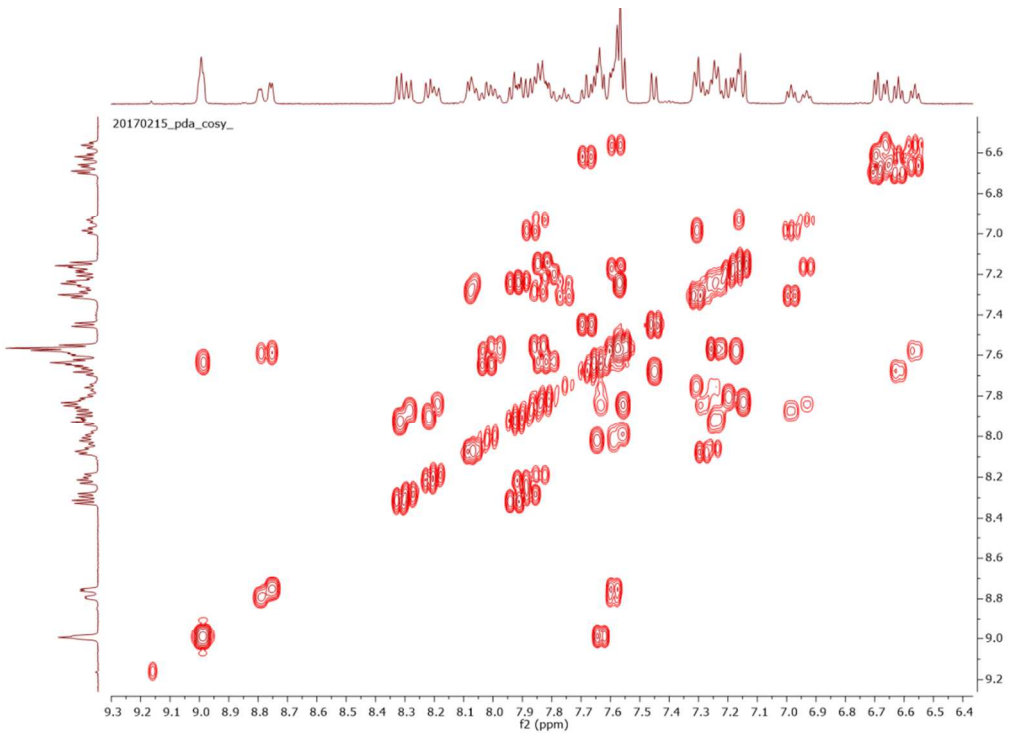


Figure S 25. ^1H COSY NMR spectrum of \mathbf{A}^{2+} in acetonitrile- d_3 at $-30\text{ }^\circ\text{C}$.

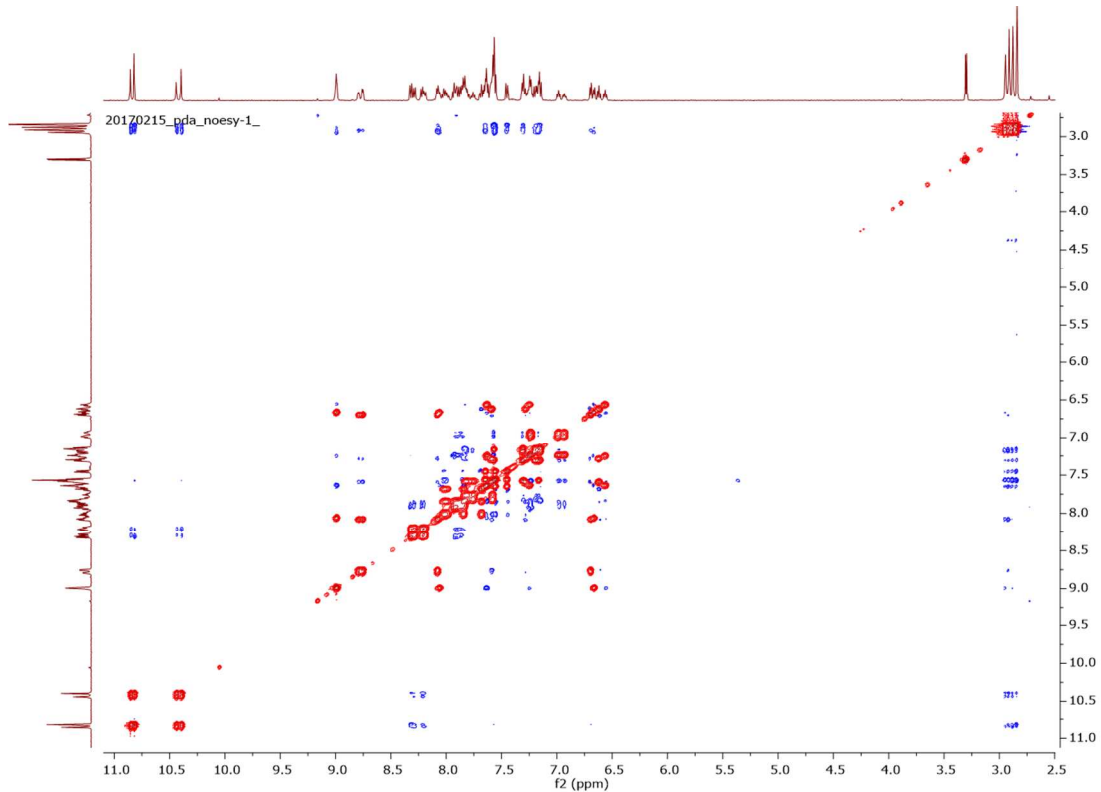


Figure S 26. 2D NOESY NMR spectrum of \mathbf{A}^{2+} in acetonitrile- d_3 at $-30\text{ }^\circ\text{C}$ (exchange peak: red colour, cross peak: blue colour).

b. Computational section

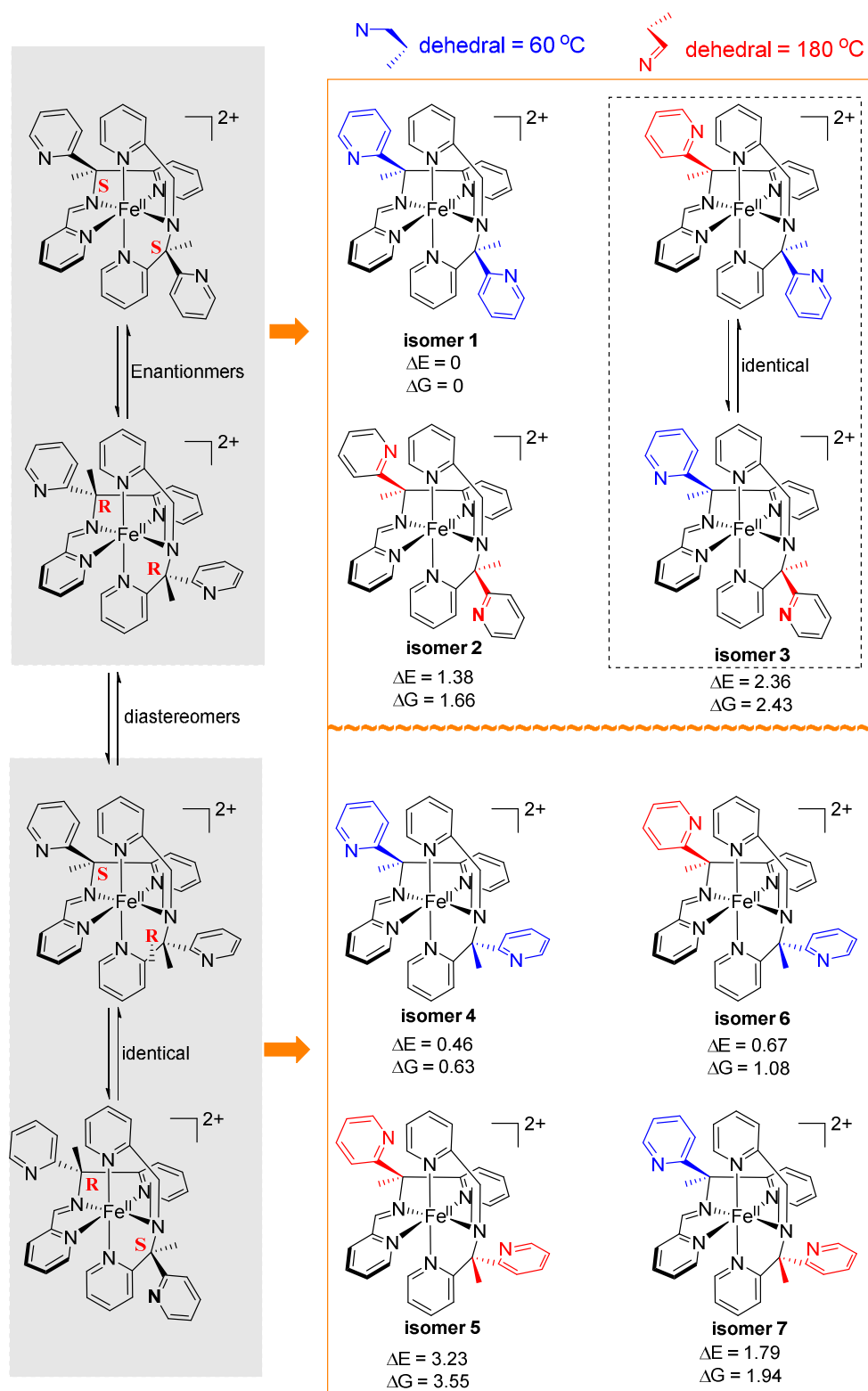
Computational details:

All Density Functional Theory (DFT) calculations were performed with the Amsterdam Density Functional (ADF) program (ADF 20016.01).¹⁰ MOs were expanded in an uncontracted set of Slater type orbitals (STOs) of triple-zeta quality containing diffuse functions (TZ2P)¹¹ and two sets of polarization functions with all electrons treated explicitly. An auxiliary set of s, p, d, f, and g STOs were used to fit the molecular density and to represent the Coulomb and exchange potentials accurately for each SCF cycle.

Geometries were optimized until the maximum gradient component was less than 10^{-4} a.u. (default value is 10^{-3} a.u.). All calculations were performed using the S12g¹² Density Functional Approximation (DFA), proven to be good for structural data, thermodynamics and spin state energetics.^{13,14,15} For all calculations, the Becke grid of verygood quality was used. COSMO dielectric continuum model was used for implicit treatment of the environment (with acetonitrile as a solvent)¹⁶. Scalar relativistic corrections have been included self-consistently by using the zeroth-order regular approximation (ZORA)^{17,18,19}. Nature of stationary points were confirmed by calculating analytical Hessians, with S12g/COSMO level of theory and integration 6 accint (Voronoi quadrature scheme).

Results and discussion:

Stereochemical considerations of bidentate imine-based Fe(II) complex **A**, taking into account two stereogenic centers, lead to 7 distinct isomers (diastereoisomers and conformers) with respect to rotation around C*-N(Py) bond (Scheme S 2). DFT calculations, revealed that all seven isomers are true minima on potential energy surface. Although isomer 1 is the global minimum (Table S1), isomers 4, 6 and 2 are close in energy, while the remaining three are higher, and thus unlikely to be detected in the reaction mixture. Furthermore, we performed separate optimizations for the three possible spin states (low, intermediate, high), which indicated clearly that the low-spin S=0 spin-state is in all cases the spin ground state, with the other spin states around 20 kcal·mol⁻¹ higher in energy (Table S2).



Scheme S 2. Schematically representation the origin of 7 different isomers of \mathbf{A}^{2+} .

Table S1. Relative energies of 7 isomers of \mathbf{A}^{2+} (kcal/mol)

Structure	Electronic energy	Gibbs free energy
Isomer 1	0	0
Isomer 2	1.38	1.66
Isomer 3	2.36	2.43
Isomer 4	0.46	0.63
Isomer 5	3.23	3.55
Isomer 6	0.67	1.08
Isomer 7	1.79	1.94

Table S2. Relative spin state energetics of 7 isomers of \mathbf{A}^{2+} (kcal/mol)

Structure	LS	IS	HS
Isomer 1	0	21.86	22.65
Isomer 2	0	18.98	19.03
Isomer 3	0	20.07	19.98
Isomer 4	0	21.46	22.10
Isomer 5	0	18.21	17.75
Isomer 6	0	19.81	22.11
Isomer 7	0	20.00	20.12

c. Mechanistic considerations

The formation of imines from pyridyl-CH₂-amine motifs has been reported to occur by reaction with singlet oxygen,^{14,20–22} generated for example by the photosensitizer (porphyrin derivatives,^{14,21} gold catalysts,²² and C₇₀ and C₆₀²⁰). In the present system irradiation of mixtures of **1** and the singlet oxygen sensitizer [Ru(bpy)₃]²⁺ (bpy = 2,2'-bipyridine) at 455 nm^{23,24} did not result in formation of \mathbf{A}^{2+} (**Figure S 27**). Furthermore, addition of potassium superoxide directly to **1** in methanol (with and without Et₃N) also did not result in the formation of \mathbf{A}^{2+} . The direct involving of singlet oxygen and superoxide as the reactive species can be excluded. Irradiation of Fe^{II} complex **1a** in air equilibrated methanol with Et₃N resulted in a slow increase in absorbance at 575 nm of \mathbf{A}^{2+} (**Figure S 29**), the rate, however, is substantially lower compared with that with the Fe^{III} complex **1** (35 min for only 50% conversion of **1a** vs 5 mins for full conversion for **1**). The lower rate is not due directly to photo-induced ligand degradation of **1a**, but the slow initial photo-oxidation of **1a** to **1**, which has been reported by our group earlier,⁴ followed by the fast photo-induced ligand oxidation from **1** (see Scheme S 3). This conclusion is supported by the absence of

photochemistry under oxygen free conditions (**Figure S 29**). Therefore, it can be concluded that Fe^{III} state bearing MeN4Py ligand is essential for the selective ligand degradation.

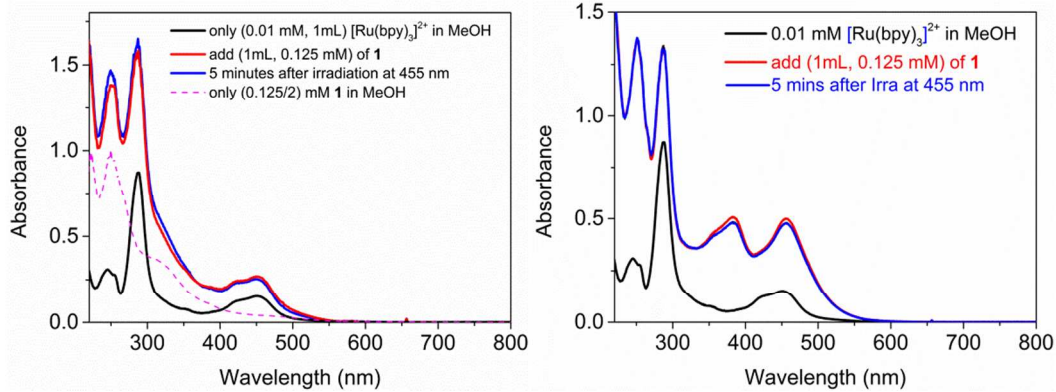


Figure S 27. UV-vis absorption spectra of **1** (left) and **1a** (right) under irradiation ($\lambda = 455$ nm) in the presence of $[\text{Ru}(\text{bpy})_3]^{2+}$.

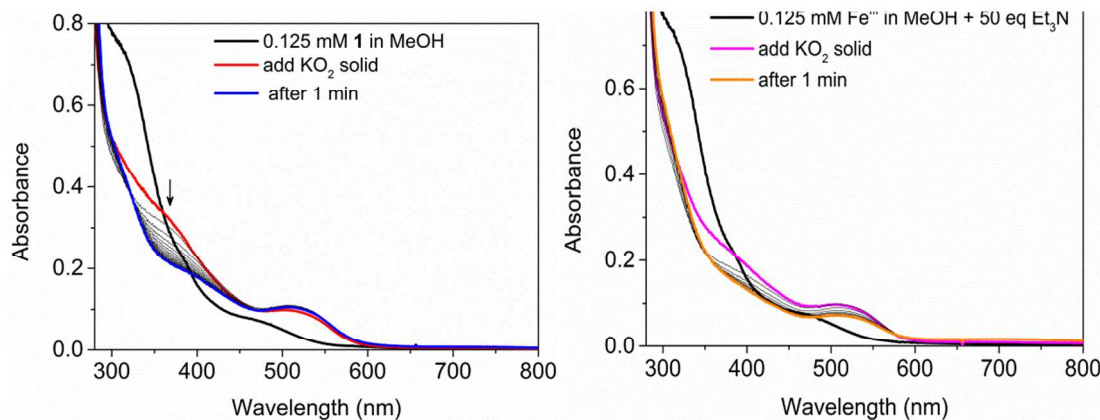


Figure S 28. UV-vis absorption spectrum of **1** before (black) and after addition of KO₂ in air equilibrated methanol without (left) and with (right) Et₃N.

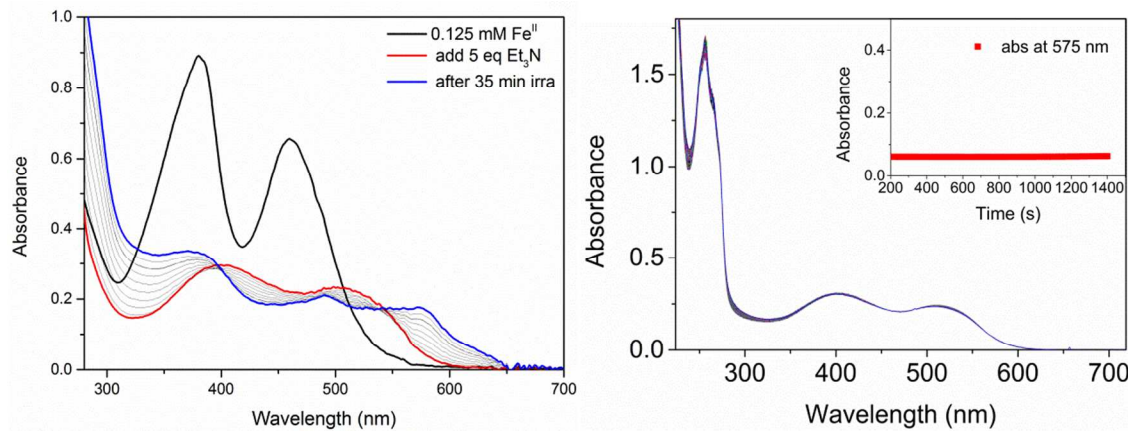
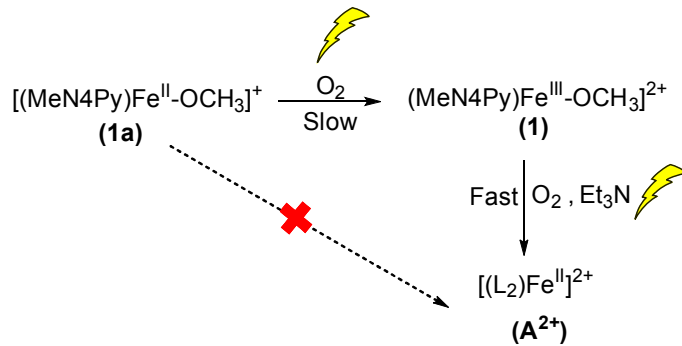


Figure S 29. UV-vis absorption spectrum of **1a** under irradiation at air equilibrated (left) and deoxygenated (right) methanol ($\lambda = 365$ nm) with Et₃N.



Scheme S 3. Mechanism for formation of photo-product **A**²⁺ by irradiation of **1a** in air equilibrated methanol with present of Et₃N.

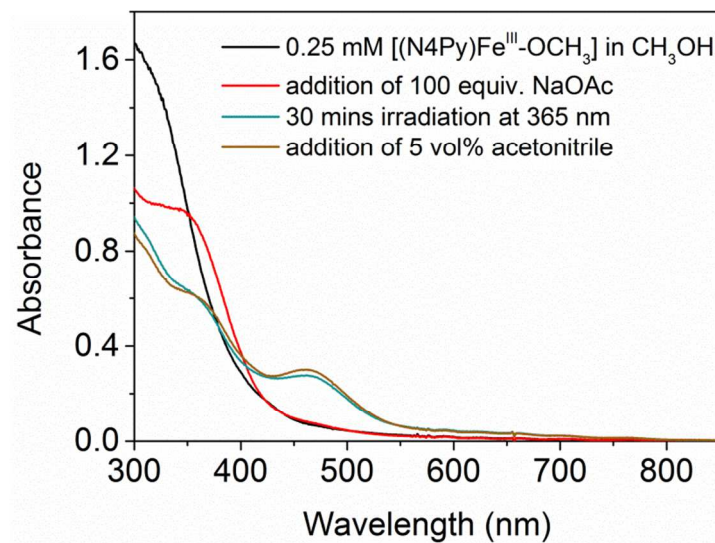


Figure S 30. UV-vis absorption spectrum of $[(\text{N4Py})\text{Fe}^{\text{III}}\text{-OCH}_3]^{2+}$ (**2**) in methanol under irradiation with present of 100 equiv. NaOAc .(The amount of corresponding $[(\text{N4Py})\text{Fe}^{\text{II}}(\text{CH}_3\text{CN})]^{2+}$ was calculated by the absorbance coefficient $\epsilon_{458\text{nm}} = 6520 \text{ M}^{-1}\times\text{cm}^{-1}$).

d. Coordinates and electronic energies (in kcal/mol) of all optimized structures

Isomer 1

-11858.1121

Fe	-0.002360	-0.054458	0.001824
N	-0.608407	1.727659	-0.552897
C	-1.656239	2.429778	-0.110447
H	-2.255280	1.971398	0.666035
N	1.438558	0.395563	-1.128944
C	-1.972535	3.685212	-0.605914
H	-2.842941	4.202512	-0.215920
N	1.013996	-1.742348	0.155812
N	-1.072742	-1.024652	-1.345508
C	-1.171140	4.252826	-1.589709
H	-1.404660	5.229949	-2.000345
N	-1.441900	-0.555084	1.112544
C	-0.054543	3.555929	-2.021540
H	0.621494	3.967530	-2.764007
N	0.653872	0.697047	1.692349
C	0.211087	2.302288	-1.480014
C	1.367501	1.513707	-1.784975
H	2.122165	1.853291	-2.485744
C	2.580984	-0.529500	-1.235763
C	2.079518	-1.836150	-0.668678
C	2.709431	-3.050205	-0.892074
C	2.273558	-4.185857	-0.224452
C	1.224989	-4.067049	0.674639
H	0.862610	-4.915154	1.245635
C	0.619145	-2.833670	0.828963
H	-0.211798	-2.704951	1.509966
C	-0.704283	-1.257677	-2.614190
H	0.137388	-0.686629	-2.983381
C	-1.347864	-2.176903	-3.422343
H	-1.004823	-2.325358	-4.440620
C	-2.407562	-2.898968	-2.895645
H	-2.921964	-3.649094	-3.487837
C	-2.817205	-2.629264	-1.597472
H	-3.668801	-3.149414	-1.175141
C	-2.149752	-1.671852	-0.850338
C	-2.615942	-1.211558	0.510430
C	-1.341014	-0.308690	2.383231
H	-2.091185	-0.587363	3.114929
C	-0.156995	0.408935	2.751098
C	0.139968	0.832232	4.042779
H	-0.529574	0.568864	4.855180
C	1.277884	1.592412	4.257037
H	1.534468	1.932393	5.255335
C	2.071118	1.928347	3.166105
H	2.957923	2.543354	3.278406
C	1.724891	1.468119	1.905103
H	2.318184	1.726071	1.037094

H	3.553205	-3.105813	-1.569544
H	2.759509	-5.141450	-0.393925
C	-3.151567	-2.354992	1.364540
H	-4.030543	-2.797947	0.894824
H	-2.399762	-3.135489	1.496364
H	-3.468564	-1.984362	2.338640
C	-5.217747	1.219400	-0.935509
C	-5.670401	1.772332	0.252159
C	-4.226785	0.245096	-0.895270
C	-5.108956	1.316648	1.440357
H	-6.438396	2.539554	0.266253
C	-3.727794	-0.145856	0.343528
H	-3.860877	-0.183709	-1.820386
N	-4.161667	0.381245	1.485978
H	-5.430927	1.722270	2.398356
C	3.722833	0.016272	-0.342563
C	4.194166	-0.654335	0.782000
C	5.182360	1.750046	-0.006696
C	5.212105	-0.070179	1.526944
H	3.785844	-1.608948	1.091098
C	5.719549	1.157305	1.131039
H	5.548075	2.714657	-0.355480
H	5.594339	-0.572935	2.410725
H	6.511033	1.651248	1.686266
N	4.207976	1.194962	-0.725737
C	3.090233	-0.668895	-2.665918
H	3.439040	0.292785	-3.040119
H	3.943142	-1.347752	-2.698889
H	2.312551	-1.058585	-3.325503
H	-5.621881	1.542613	-1.890547

Isomer 2

-11856.7307

Fe	-0.003755	-0.037984	0.011450
N	-0.340889	1.808943	-0.596944
C	-1.448442	2.539542	-0.441707
H	-2.300474	2.041669	0.013594
N	1.646211	0.303285	-0.842482
C	-1.529612	3.853849	-0.881064
H	-2.453063	4.403552	-0.731245
N	0.983609	-1.676890	0.568766
N	-1.026137	-0.637497	-1.590810
C	-0.435838	4.437195	-1.509179
H	-0.479017	5.463224	-1.860859
N	-1.654481	-0.429330	0.841547
C	0.711533	3.681566	-1.687269
H	1.589680	4.084340	-2.181557
N	0.375751	0.670088	1.812724
C	0.733665	2.371395	-1.221334

C	1.843746	1.477563	-1.355834
H	2.763309	1.766629	-1.858918
C	2.641873	-0.782200	-0.958838
C	2.241595	-1.787775	0.095510
C	3.098460	-2.791035	0.520594
C	2.672354	-3.697844	1.477357
C	1.396480	-3.550758	2.003476
H	1.016872	-4.210127	2.776842
C	0.594261	-2.530191	1.532504
H	-0.391930	-2.375860	1.947752
C	-0.647985	-0.457519	-2.868730
H	0.345727	-0.063212	-3.029570
C	-1.469489	-0.735324	-3.943379
H	-1.098279	-0.576111	-4.950270
C	-2.753227	-1.204278	-3.702311
H	-3.426335	-1.438124	-4.521236
C	-3.167194	-1.342405	-2.387530
H	-4.174659	-1.671117	-2.153505
C	-2.291132	-1.041643	-1.356266
C	-2.681595	-1.186456	0.096485
C	-1.826081	-0.065599	2.074330
H	-2.744108	-0.240601	2.630066
C	-0.690341	0.580611	2.659245
C	-0.637133	1.063111	3.962564
H	-1.509554	0.967145	4.600773
C	0.533289	1.652746	4.411939
H	0.600769	2.040291	5.423597
C	1.618549	1.729179	3.547270
H	2.559188	2.170071	3.860598
C	1.505581	1.226224	2.258317
H	2.348527	1.233284	1.572453
H	4.100539	-2.847952	0.107908
H	3.330415	-4.490500	1.819504
C	-2.587644	-2.672759	0.447433
H	-3.325847	-3.234799	-0.126500
H	-1.606611	-3.062724	0.179602
H	-2.764369	-2.839834	1.512407
C	-6.388394	-0.770791	0.947662
C	-6.525961	0.572312	0.638415
C	-5.143499	-1.376082	0.801516
C	-5.398077	1.260459	0.200630
H	-7.479573	1.082830	0.732773
C	-4.078467	-0.610477	0.339921
H	-5.028109	-2.426208	1.041600
N	-4.206471	0.688999	0.050695
H	-5.457098	2.320153	-0.045352
C	4.057354	-0.259076	-0.706589
C	5.090535	-0.397117	-1.627049
C	5.441109	0.795833	0.787628
C	6.352628	0.085891	-1.293494
H	4.936809	-0.873032	-2.588106
C	6.538994	0.691023	-0.061600
H	5.540106	1.270642	1.763177
H	7.176192	-0.015781	-1.994499
H	7.507475	1.076977	0.241763
N	4.232375	0.334088	0.479455

C	2.501716	-1.471821	-2.317583
H	2.674831	-0.771485	-3.137855
H	3.221262	-2.288661	-2.391600
H	1.508156	-1.906361	-2.419515
H	-7.237092	-1.351480	1.297818

Isomer 3

-11855.7527

Fe	0.072832	-0.015451	-0.122684
N	-0.380250	1.762660	-0.865480
C	-1.485376	2.486718	-0.671824
H	-2.265737	2.031600	-0.071078
N	1.640756	0.299397	-1.134452
C	-1.662749	3.734739	-1.253471
H	-2.584717	4.276002	-1.067756
N	1.028492	-1.700459	0.276592
N	-1.034992	-0.818562	-1.555243
C	-0.666941	4.261658	-2.066345
H	-0.786574	5.234063	-2.533792
N	-1.479349	-0.379704	0.887683
C	0.482949	3.517648	-2.274459
H	1.291001	3.878979	-2.902456
N	0.606153	0.840029	1.562491
C	0.601117	2.274373	-1.661958
C	1.732315	1.409836	-1.800314
H	2.589972	1.677645	-2.407813
C	2.718971	-0.706201	-1.131668
C	2.118750	-1.929076	-0.488020
C	2.723401	-3.174847	-0.525183
C	2.262955	-4.187213	0.304587
C	1.240757	-3.898084	1.195418
H	0.884325	-4.627517	1.914680
C	0.649740	-2.648762	1.145818
H	-0.154979	-2.390360	1.819826
C	-0.685031	-0.908595	-2.849116
H	0.331300	-0.629087	-3.094812
C	-1.563812	-1.315724	-3.834578
H	-1.221653	-1.373855	-4.862448
C	-2.868090	-1.630255	-3.479606
H	-3.589169	-1.944785	-4.227694
C	-3.234498	-1.534798	-2.146239
H	-4.244479	-1.772414	-1.827980
C	-2.299525	-1.134134	-1.205503
C	-2.596055	-1.138576	0.277756
C	-1.505428	0.010822	2.125397
H	-2.348507	-0.158741	2.790877
C	-0.333787	0.718388	2.545186
C	-0.154920	1.275814	3.807504
H	-0.928498	1.149425	4.557960
C	1.002668	1.989326	4.070564
H	1.166520	2.434087	5.046863
C	1.940753	2.138601	3.055584
H	2.854543	2.703531	3.207500
C	1.704903	1.556520	1.820082

H	2.413355	1.669188	1.008918	C	2.294949	-2.469541	-2.958571
H	3.579640	-3.341494	-1.168409	C	2.219701	-2.914677	-4.273375
H	2.726474	-5.168399	0.283391	C	2.322514	-1.995685	-5.305607
C	-2.563321	-2.605236	0.721001	H	2.259593	-2.298610	-6.346287
H	-3.429305	-3.127657	0.311892	C	2.506658	-0.658150	-4.971553
H	-1.676304	-3.103400	0.335453	H	2.590941	0.101496	-5.747352
H	-2.578434	-2.694419	1.809245	C	-0.743581	-1.050125	-2.762449
C	-6.089389	-0.415547	1.658212	H	0.065906	-0.415100	-3.093027
C	-6.282630	0.839914	1.105406	C	-1.399374	-1.880068	-3.653396
C	-4.898638	-1.090448	1.408367	H	-1.089179	-1.894740	-4.692833
C	-5.260818	1.373258	0.326421	C	-2.424761	-2.685217	-3.183752
H	-7.198439	1.399341	1.270234	H	-2.942775	-3.373806	-3.843690
C	-3.938638	-0.480941	0.605839	C	-2.809646	-2.561890	-1.855917
H	-4.743615	-2.073217	1.836858	H	-3.654730	-3.125075	-1.477679
N	-4.120205	0.733939	0.080317	C	-2.139730	-1.677584	-1.025862
H	-5.364726	2.360433	-0.122921	C	-2.636742	-1.307293	0.349542
C	3.856340	-0.173953	-0.220080	C	-1.467241	-0.385830	2.279025
C	4.156664	-0.725206	1.022937	H	-2.253564	-0.672909	2.968730
C	5.469614	1.434958	0.030889	C	-0.294151	0.313015	2.712762
C	5.169551	-0.149443	1.780977	C	-0.027650	0.673422	4.029966
H	3.620910	-1.580576	1.415912	H	-0.739408	0.412854	4.806608
C	5.843630	0.953421	1.280888	C	1.143563	1.355263	4.316547
H	5.969035	2.300284	-0.402366	H	1.378288	1.642132	5.336659
H	5.418245	-0.560963	2.755019	C	2.008560	1.668833	3.274320
H	6.638596	1.436352	1.840855	H	2.933123	2.208559	3.449394
N	4.500224	0.887111	-0.700561	C	1.685445	1.280553	1.982987
C	3.259477	-0.979755	-2.529676	H	2.334802	1.516675	1.148016
H	3.688126	-0.074667	-2.958077	H	2.196905	-3.181433	-2.148135
H	4.058786	-1.720886	-2.487261	H	2.069676	-3.970436	-4.480647
H	2.472154	-1.358893	-3.183949	C	-3.120642	-2.517291	1.138697
H	-6.853934	-0.875207	2.278017	H	-3.966674	-2.984087	0.632725
				H	-2.326203	-3.259740	1.236994
				H	-3.467489	-2.217901	2.126724
				C	-5.165282	1.239700	-1.026389

Isomer 4

-11857.6467

Fe	-0.037090	-0.079301	-0.043534	C	-5.295984	1.022902	1.340233
N	-0.649385	1.723865	-0.523429	H	-6.527385	2.379877	0.207132
C	-1.711647	2.394371	-0.066549	C	-3.779690	-0.270439	0.209114
H	-2.343354	1.879534	0.646228	H	-3.698280	-0.021236	-1.944669
N	1.429795	0.439638	-1.112369	N	-4.335359	0.100112	1.360346
C	-2.002044	3.689560	-0.466204	H	-5.722234	1.294184	2.304970
H	-2.882242	4.180869	-0.064876	C	2.350986	-1.571862	-0.263175
N	2.587070	-0.226622	-3.714111	C	3.344829	-2.472656	0.087746
N	-1.067154	-0.981829	-1.462582	C	0.841174	-2.656177	1.120504
C	-1.160565	4.330670	-1.367667	C	3.062571	-3.503026	0.971788
H	-1.370446	5.342608	-1.699196	H	4.332960	-2.382972	-0.348409
N	-1.502196	-0.627710	1.003445	C	1.777999	-3.605185	1.483378
C	-0.034430	3.661146	-1.817682	H	-0.159181	-2.683439	1.531473
H	0.671275	4.127125	-2.497688	H	3.832996	-4.216424	1.246683
N	0.568419	0.605440	1.697975	H	1.496120	-4.398587	2.167160
C	0.205367	2.365338	-1.371375	N	1.113808	-1.652089	0.272006
C	1.374792	1.602118	-1.689417	C	3.899315	0.208826	-1.138972
H	2.146119	1.984498	-2.348551	H	3.990987	0.645954	-0.142852
C	2.555279	-0.496804	-1.303632	H	4.719505	-0.495085	-1.285043
C	2.480206	-1.110121	-2.723857	H	4.008394	0.989195	-1.891594

H -5.476188 1.685567 -1.966853

Isomer 5

-11854.8770

Fe 0.001163 -0.072731 -0.135662
N -0.455668 1.684142 -0.926256
C -1.558832 2.413174 -0.737784
H -2.336106 1.969007 -0.121223
N 1.565913 0.223237 -1.164957
C -1.735555 3.652696 -1.337919
H -2.653196 4.201182 -1.151743
N 2.323918 -1.576352 -3.368331
N -1.163789 -0.896325 -1.527347
C -0.744159 4.164139 -2.166057
H -0.862602 5.131185 -2.644709
N -1.531405 -0.432295 0.920434
C 0.400361 3.411977 -2.373957
H 1.204822 3.760450 -3.013647
N 0.539087 0.843560 1.524738
C 0.519752 2.178532 -1.742435
C 1.650580 1.311872 -1.864088
H 2.503915 1.556190 -2.492398
C 2.672868 -0.751841 -1.121070
C 3.217859 -1.071042 -2.512843
C 4.549918 -0.876338 -2.864491
C 4.964375 -1.233901 -4.143794
C 4.040125 -1.763868 -5.029133
H 4.320820 -2.060608 -6.035171
C 2.726861 -1.907233 -4.592343
H 1.963960 -2.312354 -5.256401
C -0.851323 -1.006718 -2.828678
H 0.189625 -0.851983 -3.090171
C -1.786948 -1.339104 -3.791809
H -1.476474 -1.416113 -4.828810
C -3.101747 -1.558491 -3.407750
H -3.865064 -1.805168 -4.139484
C -3.421751 -1.467186 -2.061700
H -4.434430 -1.648072 -1.715600
C -2.434741 -1.144553 -1.145307
C -2.677884 -1.170168 0.346226
C -1.514806 -0.064216 2.164519
H -2.331970 -0.253443 2.856652
C -0.349951 0.671478 2.546567
C -0.150935 1.236099 3.802733
H -0.881253 1.057737 4.585397
C 0.963793 2.028915 4.015300
H 1.142979 2.481267 4.985425
C 1.832482 2.254788 2.953549
H 2.702333 2.894174 3.059508
C 1.584396 1.651239 1.730759
H 2.239033 1.824022 0.885548
H 5.268548 -0.462121 -2.167848
H 6.001827 -1.098418 -4.436045
C -2.638932 -2.643709 0.763538

H -3.499392 -3.165900 0.342897
H -1.747504 -3.128290 0.370292
H -2.656939 -2.750149 1.850555
C -6.184473 -0.486733 1.721410
C -6.319459 0.831388 1.317829
C -5.007804 -1.169712 1.428160
C -5.255619 1.415925 0.637818
H -7.221553 1.399963 1.522279
C -4.002864 -0.505431 0.731756
H -4.899052 -2.200516 1.742376
N -4.129973 0.768749 0.350149
H -5.311867 2.452559 0.307025
C 2.098769 -1.968969 -0.434500
C 2.765770 -3.182575 -0.399388
C 0.615067 -2.687037 1.181726
C 2.324038 -4.181727 0.454697
H 3.640199 -3.330545 -1.024964
C 1.251671 -3.909073 1.291235
H -0.219223 -2.441735 1.823717
H 2.829418 -5.141921 0.488613
H 0.895280 -4.630657 2.018670
N 0.985048 -1.749010 0.295886
C 3.760891 -0.222072 -0.178724
H 3.358083 -0.095854 0.825195
H 4.580064 -0.939217 -0.111767
H 4.151305 0.735419 -0.530517
H -6.983244 -0.988562 2.260080

Isomer 6

-11857.4358

Fe 0.079491 -0.006150 -0.138345
N -0.332911 1.818114 -0.759250
C -1.441777 2.531510 -0.544851
H -2.257840 2.023453 -0.036942
N 1.676324 0.349956 -1.081077
C -1.566208 3.842999 -0.982945
H -2.487117 4.380630 -0.782290
N 2.812668 -0.624983 -3.649503
N -0.993086 -0.664714 -1.674994
C -0.517259 4.440075 -1.671782
H -0.593719 5.465323 -2.020139
N -1.508717 -0.416619 0.784475
C 0.629147 3.700071 -1.912676
H 1.473361 4.115218 -2.453691
N 0.544781 0.752614 1.614770
C 0.696195 2.391939 -1.444926
C 1.815739 1.517499 -1.630691
H 2.686646 1.815669 -2.204567
C 2.678004 -0.725724 -1.228017
C 2.484464 -1.389395 -2.609818
C 1.972518 -2.674762 -2.760871
C 1.803814 -3.178040 -4.045470
C 2.147876 -2.386257 -5.130274
H 2.030711 -2.737523 -6.150913

C	2.650427	-1.114208	-4.878169
H	2.932066	-0.456496	-5.699252
C	-0.666418	-0.524247	-2.971417
H	0.324091	-0.148623	-3.185170
C	-1.538149	-0.818380	-4.001521
H	-1.209249	-0.690174	-5.027506
C	-2.816721	-1.260084	-3.692604
H	-3.529711	-1.499637	-4.475319
C	-3.172363	-1.369838	-2.357464
H	-4.170449	-1.686152	-2.072268
C	-2.246627	-1.060791	-1.373620
C	-2.553474	-1.205683	0.100239
C	-1.611012	-0.050306	2.024823
H	-2.486657	-0.244414	2.639231
C	-0.455647	0.628034	2.533476
C	-0.323342	1.113108	3.830682
H	-1.143393	0.989557	4.530511
C	0.855798	1.741440	4.195845
H	0.984465	2.127433	5.202050
C	1.869592	1.868081	3.252838
H	2.809991	2.351864	3.494150
C	1.676661	1.362663	1.976194
H	2.446984	1.445794	1.217291
H	1.699542	-3.281355	-1.905218
H	1.401326	-4.176508	-4.190281
C	-2.386092	-2.687736	0.444346
H	-3.125975	-3.279192	-0.096675
H	-1.403539	-3.037990	0.130553
H	-2.506678	-2.861475	1.516023
C	-6.226030	-0.926161	1.126491
C	-6.411630	0.424171	0.880020
C	-4.974122	-1.490135	0.900160
C	-5.324285	1.159369	0.417257
H	-7.371852	0.904860	1.040503
C	-3.951216	-0.677479	0.424057
H	-4.820219	-2.545266	1.091796
N	-4.126302	0.627659	0.190285
H	-5.422639	2.225629	0.216388
C	2.358326	-1.705507	-0.127206
C	3.262761	-2.664192	0.304819
C	0.806901	-2.428317	1.427005
C	2.912929	-3.536579	1.323135
H	4.239395	-2.732700	-0.159440
C	1.660281	-3.404595	1.902620
H	-0.162871	-2.286277	1.882523
H	3.612041	-4.293590	1.663959
H	1.336953	-4.040376	2.719812
N	1.123348	-1.607924	0.410096
C	4.100343	-0.189234	-1.104187
H	4.244211	0.301208	-0.139031
H	4.823374	-1.000304	-1.194704
H	4.312848	0.513373	-1.908886
H	-7.042032	-1.543525	1.491073

Isomer 7

-11856.3236

Fe	-0.112902	-0.140543	-0.015187
N	-0.729509	1.600726	-0.684782
C	-1.753072	2.345468	-0.254553
H	-2.329013	1.946902	0.570322
N	1.305578	0.236623	-1.206232
C	-2.068768	3.573272	-0.814929
H	-2.916967	4.127551	-0.426826
N	2.086636	-1.343307	-3.553046
N	-1.264029	-1.206327	-1.233177
C	-1.293084	4.068510	-1.856645
H	-1.525105	5.023771	-2.316565
N	-1.507441	-0.564632	1.193924
C	-0.200624	3.330058	-2.280108
H	0.458940	3.687149	-3.064377
N	0.584646	0.757278	1.594063
C	0.067410	2.108585	-1.670396
C	1.216736	1.299969	-1.943086
H	1.960107	1.581635	-2.684698
C	2.468015	-0.672785	-1.257864
C	2.984518	-0.869168	-2.684231
C	4.294214	-0.585695	-3.058922
C	4.680142	-0.818929	-4.375462
C	3.751612	-1.319269	-5.273479
H	4.011184	-1.518809	-6.308701
C	2.461800	-1.559584	-4.810425
H	1.694907	-1.945811	-5.481057
C	-0.946980	-1.556788	-2.488399
H	-0.043815	-1.128472	-2.908466
C	-1.684247	-2.477552	-3.212442
H	-1.377017	-2.724413	-4.223410
C	-2.780703	-3.078916	-2.616450
H	-3.372177	-3.820244	-3.144701
C	-3.116633	-2.707417	-1.322938
H	-3.982668	-3.141366	-0.837193
C	-2.356556	-1.757079	-0.659985
C	-2.730044	-1.217071	0.697668
C	-1.335313	-0.264500	2.444969
H	-2.042491	-0.510846	3.228891
C	-0.152783	0.494942	2.711450
C	0.182915	1.012227	3.958745
H	-0.426853	0.758010	4.819788
C	1.273447	1.859086	4.064277
H	1.559357	2.274594	5.025342
C	1.972415	2.190003	2.908822
H	2.809192	2.880018	2.931116
C	1.596350	1.625584	1.699968
H	2.118686	1.876786	0.785283
H	5.017273	-0.194175	-2.354036
H	5.699355	-0.609438	-4.687305
C	-3.241552	-2.304998	1.637037
H	-4.154079	-2.749617	1.238256
H	-2.500231	-3.095851	1.766660

H	-3.497686	-1.880615	2.607255	C	2.201091	-4.277618	-0.075415
C	-5.387528	1.191185	-0.686177	H	3.460157	-3.241222	-1.485662
C	-5.729658	1.827898	0.496424	C	1.145385	-4.128303	0.812508
C	-4.417321	0.195472	-0.664406	H	-0.300058	-2.742598	1.592372
C	-5.083033	1.430714	1.662011	H	2.694514	-5.236691	-0.198875
H	-6.476695	2.615265	0.523423	H	0.786912	-4.954615	1.417212
C	-3.826897	-0.132267	0.552340	N	0.915487	-1.829530	0.194337
H	-4.136033	-0.297861	-1.586833	C	3.560356	-0.149617	-0.318421
N	-4.155681	0.474861	1.690120	H	3.192465	-0.115372	0.705314
H	-5.317137	1.902315	2.615370	H	4.413971	-0.828847	-0.331872
C	1.972877	-1.960349	-0.634616	H	3.891329	0.847774	-0.616357
C	2.624333	-3.171293	-0.797209	H	-5.860732	1.466740	-1.624339
C	0.530625	-2.894300	0.915377				

3. References

- (1) Draksharapu, A.; Li, Q.; Logtenberg, H.; van den Berg, T. A.; Meetsma, A.; Killeen, J. S.; Feringa, B. L.; Hage, R.; Roelfes, G.; Browne, W. R. Ligand Exchange and Spin State Equilibria of $\text{Fe}(\text{N4Py})$ and Related Complexes in Aqueous Media. *Inorg. Chem.* **2011**, *51*, 900–913.
- (2) Roelfes, G.; Lubben, M.; Hage, R.; Que, Jr., L.; Feringa, B. L. Catalytic Oxidation with a Non-Heme Iron Complex That Generates a Low-Spin $\text{Fe}^{\text{II}}\text{OOH}$ Intermediate. *Chem. - A Eur. J.* **2000**, *6*, 2152–2159.
- (3) Roelfes, G.; Lubben, M.; Chen, K.; Ho, R. Y. N.; Meetsma, A.; Genseberger, S.; Hermant, R. M.; Hage, R.; Mandai, S. K.; Young Jr., V. G.; Zang, Y.; Kooijman, H.; Spek, A. L.; Que Jr., L.; Feringa, B. L. Iron Chemistry of a Pentadentate Ligand That Generates a Metastable $\text{Fe}^{\text{III}}\text{-OOH}$ Intermediate. *Inorg. Chem.* **1999**, *38*, 1929–193.
- (4) Draksharapu, A.; Li, Q.; Roelfes, G.; Browne, W. R. Photo-Induced Oxidation of $[\text{Fe}(\text{N4Py})\text{CH}_3\text{CN}]$ and Related Complexes. *Dalton Trans.* **2012**, *41*, 13180–13190.
- (5) Hatchard, C.; Parker, C. A. A New Sensitive Chemical Actinometer - II. Potassium Ferrioxalate as a Standard Chemical Actinometer. *Proc. R. Soc. London. Ser. A. Math. Phys. Sci.* **1956**, *235* (1203), 518 LP-536.
- (6) Travieso-Puente, R.; Budzak, S.; Chen, J.; Stacko, P.; Jastrzebski, J. T. B. H.; Jacquemin, D.; Otten, E. Arylazoindazole Photoswitches: Facile Synthesis and Functionalization via SNAr Substitution. *J. Am. Chem. Soc.* **2017**, *139*, 3328–3331.
- (7) Maafi, W.; Maafi, M. Modelling Nifedipine Photodegradation, Photostability and Actinometric Properties. *Int. J. Pharm.* **2013**, *456*, 153–164.
- (8) Maafi, M.; Maafi, W. Quantification of Unimolecular Photoreaction Kinetics: Determination of Quantum Yields and Development of Actinometers - The Photodegradation Case of Cardiovascular Drug Nisoldipine. *Int. J. Photoenergy* **2015**, *454895*.
- (9) Olivo, G.; Arancio, G.; Mandolini, L.; Lanzalunga, O.; Di Stefano, S. Hydrocarbon Oxidation Catalyzed by a Cheap Nonheme Imine-Based Iron(II) Complex. *Catal. Sci. Technol.* **2014**, *4*, 2900–2903.
- (10) te Velde, G.; Bickelhaupt, F. M.; Baerends, E. J.; Fonseca Guerra, C.; van Gisbergen, S. J. A.;

- Snijders, J. G.; Ziegler, T. Chemistry with ADF. *J. Comput. Chem.* **2001**, *22*, 931–967.
- (11) Van Lenthe, E.; Baerends, E. J. Optimized Slater-Type Basis Sets for the Elements 1–118. *J. Comput. Chem.* **2003**, *24*, 1142–1156.
- (12) Swart, M. A New Family of Hybrid Density Functionals. *Chem. Phys. Lett.* **2013**, *580*, 166–171.
- (13) Gruden, M.; Stepanovic, S.; Swart, M. Spin State Relaxation of Iron Complexes: The Case for OPBE and S12g. *J. Serbian Chem. Soc.* **2015**, *80*, 1399–1410.
- (14) Ushakov, D. B.; Plutschack, M. B.; Gilmore, K.; Seeberger, P. H. Factors Influencing the Regioselectivity of the Oxidation of Asymmetric Secondary Amines with Singlet Oxygen. *Chem. – A Eur. J.* **2015**, *21*, 6528–6534.
- (15) Chen, J.; Stepanovic, S.; Draksharapu, A.; Gruden, M.; Browne, W. R. A Non-Heme Iron Photocatalyst for Light Driven Aerobic Oxidation of Methanol. *Angew. Chem. Int. Ed.* **2018**, *57*, 3207–3211.
- (16) Klamt, A.; Schuurmann, G. COSMO: A New Approach to Dielectric Screening in Solvents with Explicit Expressions for the Screening Energy and Its Gradient. *J. Chem. Soc. Perkin Trans. 2* **1993**, *5*, 799–805.
- (17) Lenthe, E. van; Baerends, E. J.; Snijders, J. G. Relativistic Regular Two-component Hamiltonians. *J. Chem. Phys.* **1993**, *99*, 4597–4610.
- (18) van Lenthe, E.; Baerends, E. J.; Snijders, J. G. Relativistic Total Energy Using Regular Approximations. *J. Chem. Phys.* **1994**, *101*, 9783–9792.
- (19) van Lenthe, E.; Ehlers, A.; Baerends, E.-J. Geometry Optimizations in the Zero Order Regular Approximation for Relativistic Effects. *J. Chem. Phys.* **1999**, *110*, 8943–8953.
- (20) Kumar, R.; Gleißner, E. H.; Tiu, E. G. V.; Yamakoshi, Y. C70 as a Photocatalyst for Oxidation of Secondary Benzylamines to Imines. *Org. Lett.* **2016**, *18*, 184–187.
- (21) Jiang, G.; Chen, J.; Huang, J.-S.; Che, C.-M. Highly Efficient Oxidation of Amines to Imines by Singlet Oxygen and Its Application in Ugi-Type Reactions. *Org. Lett.* **2009**, *11*, 4568–4571.
- (22) To, W.-P.; Tong, G. S.-M.; Lu, W.; Ma, C.; Liu, J.; Chow, A. L.-F.; Che, C.-M. Luminescent Organogold(III) Complexes with Long-Lived Triplet Excited States for Light-Induced Oxidative C–H Bond Functionalization and Hydrogen Production. *Angew. Chem. Int. Ed.* **2012**, *51*, 2654–2657.

- (23) Abdel-Shafi, A. A.; Worrall, D. R.; Ershov, A. Y. Photosensitized Generation of Singlet Oxygen from Ruthenium(II) and Osmium(II) Bipyridyl Complexes. *Dalton Trans.* **2004**, 1, 30–36.
- (24) Prier, C. K.; Rankic, D. A.; MacMillan, D. W. C. Visible Light Photoredox Catalysis with Transition Metal Complexes: Applications in Organic Synthesis. *Chem. Rev.* **2013**, 113, 5322–5363.